Coronaviruses using different strategies to antagonize antiviral responses and pyroptosis

Xinyu Fu[1,6], Yang Yang[2,6], Weilv Xu[1,6], Danyue Li[1,6], Xinyue Li[1], Nan Chen[1], Qian Lv[1], Yuhua Shi[1], Xiaoliang Li[1,3,4], Jidong Xu[1,3,*], Fushan Shi[1,3,5,*]

[1] Department of Veterinary Medicine, College of Animal Sciences, Zhejiang University, Hangzhou 310058, Zhejiang, China

[2] Key Laboratory of Applied Technology on Green-Eco-Healthy Animal Husbandry of Zhejiang Province, Zhejiang Provincial Engineering Research Center for Animal Health Diagnostics & Advanced Technology, Zhejiang International Science and Technology Cooperation Base for Veterinary Medicine and Health Management, China-Australia Joint Laboratory for Animal Health Big Data Analytics, College of Animal Science and Technology & College of Veterinary Medicine of Zhejiang A&F University, Hangzhou 310058, Zhejiang, China

[3] Institute of Preventive Veterinary Medicine, Zhejiang Provincial Key Laboratory of Preventive Veterinary Medicine, Zhejiang University, Hangzhou 310058, Zhejiang, China

[4] Hainan Institute of Zhejiang University, Sanya 572025, Hainan, China

[5] Veterinary Teaching Hospital, Center for Veterinary Sciences, Zhejiang University, Hangzhou 310058, Zhejiang, China

[6] These authors contributed equally to this work

[*] Corresponding author: Jidong Xu, E-mail: jidongxu@zju.edu.cn; Fushan Shi, E-mail: sfs@zju.edu.cn

Abstract

Viral infection triggers inflammasome-mediated caspase-1 activation. However, less is known about how viruses use the active caspase-1 to evade host immune response. Here, we use porcine epidemic diarrhea virus (PEDV) as a model of coronaviruses (CoVs) to illustrate the sophisticated regulation of CoVs to counteract IFN-I signaling and pyroptosis. We show that PEDV infection stabilizes caspase-1 expression via papain-like protease PLP2's deubiquitinase activity and the enhanced stabilization of caspase-1 disrupts IFN-I signaling by cleaving RIG-I at D189 residue. Meanwhile, PLP2 can degrade GSDMD-p30 by removing its K27-linked ubiquitin chain at K275 to restrain pyroptosis. Papain-like proteases from other genera of CoVs (PDCoV and SARS-CoV-2) have the similar activity to degrade GSDMD-p30. We further demonstrate that SARS-CoV-2 N protein induced NLRP3 inflammasome activation also uses the active caspase-1 to counter IFN-I signaling by cleaving RIG-I. Therefore, our work unravels a novel antagonistic mechanism employed by CoVs to evade host antiviral response.

Keywords: Coronavirus; Papain-like protease; Antiviral immunity; GSDMD; Type I interferon signaling

Introduction

Coronaviruses which belong to order Nidovirales, family Coronaviridae, and subfamily Orthocoronavirinae, are a group of viruses packaged in envelop covered with spikes and contain a linear, single and positive-stranded RNA[1]. Coronaviruses

are subdivided into four genera, including α, β, γ, and δ. As a member of α genus, PEDV infection was characterized by vomiting, severe diarrhea, dehydration and high mortality in suckling piglets[2]. The viral genome of PEDV contains a full-length genome of 28 kb and encodes a total of seven open reading frames (ORFs)[3]. Like other CoVs, PEDV utilizes its own proteases, including papain-like protease (PLpro) and main protease to cleave the polyprotein. The papain-like protease of PEDV is encoded by the largest nonstructural protein Nsp3, which contains two papain-like protease domains (PLP1 and PLP2 or PLpro)[4]. In general, α coronaviruses and clade A of β coronaviruses harbor PLP1 and PLP2, and other coronaviruses have one functional PLpro only[5]. Studies have shown that CoVs PLP2 (PLpro) act as a viral deubiquitinase to negatively regulate type I IFN signaling pathway[4,6]. For example, mouse hepatitis virus (MHV) PLP2 can bind to and deubiquitinate IRF3 to prevent its nuclear translocation[7]. Transmissible gastroenteritis virus (TGEV) PLP2 is able to inhibit the degradation of IκBα by decreasing its ubiquitination, resulting in the suppression of NF-κB signaling[8]. As to PEDV PLP2, it has been reported that PLP2 deubiquitinates RIG-I and STING to block the IFN signaling pathway[4]. The catalytically dead mutants of PLP2 (C1729A, H1888A and D1901A) can abrogate their deubiquitinase activity and fail to inhibit PEDV-induced IFN-β production.

Caspase-1 is a cysteine protein hydrolase, which participates in cell death and inflammatory response[9]. Caspase-1 exists in the form of proteasome (pro-caspase-1) at static state and acts as an enzyme after activation, which relies on the activation of different inflammasomes[10]. Interestingly, high expression of pro-caspase-1 can also

result in its auto-activation in the absence of a ligand[11-13]. Pyroptosis is an inflammatory caspases-dependent, pro-inflammatory programmed cell death characterized by losing of cell membrane integrity, pore forming and swelling and rupture of the cells[14]. The canonical pathway of pyroptosis is mediated by caspase-1[15,16]. When host cells' pattern-recognition receptors (PRRs) are stimulated by pathogen-associated molecular patterns (PAMPs) or damage-associated molecular patterns (DAMPs), inflammasomes will assemble automatically and activate themselves, leading to the activation of caspase-1. Researches have demonstrated that NLRP3 inflammasome can be activated by ZIKA[17], SARS-CoV-2[18] and MERS-CoV[19,20], and AIM2 inflammasome can be activated by SARS-CoV-2[21] while NLRP1 inflammasome can be activated by human rhinovirus (HRV) and picornaviruses[22]. Activated caspase-1 cleaves GSDMD to produce N-terminal GSDMD-p30 fragments with perforating activity on cell membrane, which leads to pyroptosis, and it also cleaves pro-IL-1β to produce IL-1β to improve antiviral capacity[15,16].

What is clear is that, inflammasomes-mediated caspase-1 activation and pyroptosis induced by viruses will lead to enhancement of cell antiviral capability and destruction of cell integrity, and these changes are detrimental to virus replication, especially at the early stage of viral infection. So what is the purpose of viral activation of caspase-1 as well as pyroptosis? Here, we report that PEDV infection increases the stabilization of caspase-1 by removing its K11-linked ubiquitin chains at K134 via its papain-like protease PLP2. Consequently, caspase-1 targets to RIG-I for

cleavage at D189 residue which leads to decreased IFN-I signaling and enhanced PEDV replication. Meanwhile, to assure the integrity of host cells which might be broken by GSDMD-p30 cleaved by caspase-1, PLP2 can degrade GSDMD-p30 by removing its K27-linked ubiquitin chain at K275 residue to restrain pyroptosis. We further demonstrate that papain-like proteases from other genera of CoVs, such as PDCoV and SARS-CoV-2, have the similar activity to degrade GSDMD-p30. Importantly, we confirm that SARS-CoV-2 N protein induced NLRP3 inflammasome activation also uses the active caspase-1 to counter IFN-I signaling. Therefore, our findings uncover a distinctive feature of papain-like protease in antagonizing antiviral responses that might serve as a target for CoVs treatment in the future.

Results

PEDV infection elevates the expression of caspase-1

In order to investigate the effect of PEDV on porcine caspase-1, endogenous caspase-1 expression was analyzed by immunoblotting in intestinal tissues of mock-infected and PEDV naturally-infected piglets. The results showed that expression of caspase-1 was increased in the PEDV-infected piglets (Fig. 1A). qRT-PCR showed that *caspase-1* mRNA abundance was not altered in IPEC-J2 cells upon PEDV infection (Fig. 1B). Immunoblotting also confirmed that PEDV infection promoted the amount of caspase-1 in IPEC-J2 cells and CHX treatment further elevated caspase-1 expression (Fig. 1C), suggesting that the increased caspase-1 expression was not caused by the transcription of mRNA and synthesis of new

proteins. In addition, Vero cells were transfected with plasmids encoding caspase-1 and then infected with PEDV. We found that the increased caspase-1 by PEDV infection was both MOI and time dependent (Fig. 1D and E). Since the high expression of caspsae-1 causes auto-activation and produces active caspase-1 p20[11-13], which can lead to the cleavage of GSDMD, we investigated the relationship between PEDV infection and pyroptosis. Vero cells were co-transfected with GSDMD-FL (full length) and caspase-1 and then infected with PEDV. Caspase-1 expression and cleavage of GSDMD increased progressively in both MOI and time dependent manner during infection (Fig. 1F and G). Interestingly, PEDV infection resulted in declines in LDH release compared to mock-infected group, despite the increased GSDMD cleavage (Fig. 1H and I). These results indicate that PEDV infection promotes the amount of caspase-1.

The papain-like protease 2 of PEDV inhibits the proteasomal degradation of caspase-1

The increased expression of caspase-1 induces GSDMD cleavage but inhibits pyroptosis. Therefore, we speculated that some kind of viral proteins affected this process. Vero cells transfected with GSDMD-FL were infected with PEDV, following performed with coimmunoprecipitation (Co-IP) and mass spectrometry (MS) analysis. The database search revealed that the papain-like protease 2 (PLP2) of PEDV binds to GSDMD-FL during infection (Supplementary Fig. 1A). The Co-IP assay also confirmed that PEDV PLP2 interacted with GSDMD-FL (Supplementary Fig. 1B).

Since it is known that GSDMD-FL and caspase-1 are interacted[23], we further examined whether PLP2 interacts with caspase-1. HEK293T cells were co-transfected with FLAG-tagged caspase-1 and MYC-tagged PLP2, following treated with VX765, an inhibitor of caspase-1, to curb caspase-1 activation. Co-IP assay showed that PLP2 interacted with caspase-1 (Supplementary Fig. 1C). Indirect immunofluorescence further demonstrated that GSDMD, caspase-1 and PEDV PLP2 were colocalized in the cytoplasm (Supplementary Fig. 1D). Thus, PLP2 interacts with both caspase-1 and GSDMD.

Given that high expression of caspase-1 leads to auto-activation, caspase-1-C285A (caspase-1 mutant, which lacks its protease activity) and PLP2 were co-transfected into HEK293T cells. As shown in Fig. 2A, we observed an increased protein amount of caspase-1-C285A in the presence of PLP2. In addition, co-transfection of PLP2, GSDMD-FL and caspase-1 in HEK293T also revealed that PLP2 caused the accumulation of caspase-1 but not GSDMD-FL (Supplementary Fig. 2A). We next measured caspase-1 degradation by a cycloheximide (CHX) chase assay to determine whether PLP2 could stabilize caspase-1. The results demonstrated that PEDV PLP2 could stabilize caspase-1 but not GSDMD-FL by delaying its degradation (Fig. 2B and Supplementary Fig. 2B). Ubiquitination is a key signal for proteasomal degradation, and PLP2 has the deubiquitinase activity. To identify whether the deubiquitinase activity of PLP2 is required for the stabilization of caspase-1, we generated the catalytic mutants (C113A, H272A, D285A) of PLP2 and co-transfected them with caspase-1-C285A. As expected, all of the three mutants lost the ability to

stabilize caspase-1 (Fig. 2C). Furthermore, we co-expressed the wild type PLP2 or its mutants with HA-tagged ubiquitin (HA-Ub) and FLAG-tagged caspase-1 in HEK293T cells. Compared to the empty vector, wild type PLP2 substantially inhibited ubiquitination of caspase-1 while the three mutants had no effect on it (Fig. 2D), suggesting that the deubiquitinase activity of PLP2 is indispensable for the stabilization of caspase-1.

It has been reported that the K11-linked ubiquitination of human caspase-1 at Lys-134 is a way to induce its degradation[24]. To determine whether K134 residue of porcine-derived caspase-1 is also critical for its ubiquitination, we constructed porcine-derived caspase-1-K134R mutant in which the lysine (K) residue was replaced with arginine (R). As shown in Fig. 2E, wild type caspase-1 was degraded by K11 in a dose-dependent manner, while caspase-1-K134R could not be degraded by K11. Moreover, we found that caspase-1-K134R mutant exhibited a dramatic decrease in K11-linked ubiquitination (Supplementary Fig. 2C). To further confirm the role of PLP2 in this process, we co-expressed PLP2 with caspase-1 and K11 ubiquitin, the results demonstrated that the degradation effect of K11 on caspase-1 was abrogated by PLP2 (Fig. 2F). Immunoblotting also showed that PLP2 stabilized caspase-1 but not caspase-1-K134R (Fig. 2G). Additionally, PEDV infection decreased K11-linked poly-ubiquitination of caspase-1, further fortifying the above findings (Fig. 2H). Taken together, these results indicate that PLP2 of PEDV stabilizes porcine caspase-1 by removing K11-linked ubiquitin chains at Lys134.

177 **Caspase-1 attenuates IFN-I signaling during PEDV infection**

178 It has been reported that caspase-1 can negatively regulate IFN-I signaling by
179 cleaving cGAS during DNA virus infection[25]. As an RNA virus, PEDV activates
180 IFN-I signaling through the RLRs pathway. Since IFN-I plays a vital role in antiviral
181 process, we wondered whether the stabilized caspase-1 can affect it. We initially
182 found that overexpression of caspase-1 in IPEC-J2 cells attenuated the *IFN-α*, *IFN-β*,
183 *ISG15* and *OAS1* mRNA levels induced by poly (I:C) treatment (Fig. 3A-D). In
184 addition, caspase-1 inhibitor VX765 reversed the attenuated IFN-I signaling during
185 poly (I:C) treatment (Fig. 3E and F). Moreover, knockout of caspase-1 in THP-1 cells
186 further promoted the expression of *IFN-β* and *ISG15* mRNA induced by poly (I:C)
187 (Fig. 3G and H). Same results were observed for PLP2 in IPEC-J2 cells (Fig. 3I and J).
188 Thus, we determined that both caspase-1 and PLP2 were antagonists of IFN-I. Next,
189 the above-mentioned findings were further verified in PEDV-infected IPEC-J2 cells,
190 which were consistent with our observations (Fig. 3 K-P). These results indicate that
191 PEDV-induced IFN-I signaling was counteracted by the stabilized caspase-1.

192 The role of caspase-1 and PLP2 in viral replication was further analyzed
193 considering the vital antiviral effect of IFN-I. PLP2 was transfected into IPEC-J2 cells
194 and then infected with PEDV. Consistent with its antagonistic effect on IFN-I, the
195 results showed that PLP2 could promote PEDV replication, which was also confirmed
196 by immunoblotting (Fig. 3Q). Since the high expression of caspase-1 leads to
197 autoprocessing, we transfected caspase-1 with different doses and then treated with
198 PEDV infection. As shown in Fig. 3R, all doses of caspase-1 could promote PEDV

199 replication, while the effect of high concentration of caspase-1 was attenuated, which
200 might relate to pyroptosis caused by caspase-1 activation. Moreover, the use of
201 VX765 inhibited viral replication co-treated with necrosulfonamide (NSA), a specific
202 GSDMD inhibitor (Fig. 3S). Together, these data suggest that the enhanced caspase-1
203 stabilized by PEDV infection attenuates type I IFN signaling and thus benefits to viral
204 replication.
205
206 **Cleavage of RIG-I by caspase-1 ensures PEDV replication**
207 As caspase-1 is vital to suppress type I IFN during PEDV infection, we hypothesized
208 that caspase-1 exerted its effect on RIG-I. Therefore, we analyzed whether caspase-1
209 could directly interact with RIG-I. HEK293T cells were then transfected with
210 MYC-tagged RIG-I and FLAG-tagged caspase-1, Co-IP assay showed that RIG-I
211 interacted with caspase-1 (Fig. 4A). Interestingly, we found that RIG-I was
212 diminished after co-transfected with caspase-1 (Fig. 4B). Thus, we co-transfected
213 caspase-1 or its mutant with RIG-I at different doses in HEK293T, followed with
214 immunoblotting. As shown in Fig. 4C, a clear band with a molecular weight around
215 25-35 kDa was observed, while the caspase-1-C285A (caspase-1 mutant) impaired the
216 cleavage. Because RIG-I was N-terminal MYC-tagged, we speculated that caspase-1
217 cut RIG-I at N-terminus. We therefore generated mutants of RIG-I at different sites to
218 identify the exact cleavage site of RIG-I by caspase-1. RIG-I or its mutants (D163A,
219 D189A, D194A, D199/202/203A and D209A) were co-transfected with caspase-1 in
220 HEK293T cells. As shown in Fig. 4D and Supplementary Fig. 3A, wild-type RIG-I,

D163A, D194A, D199/202/203A and D209A could still be cleaved by caspase-1 successfully, while RIG-I-D189A could not be cleaved. These results imply that RIG-I was a cleaved target of caspase-1 at D189. Moreover, we investigated the relationship between human derived caspase-1 and RIG-I. As shown in Supplementary Fig. 3B, a band with a molecular weight around 25-35 kDa was observed (lane 2). Based on the multiple-sequence alignment of RIG-Is (Supplementary Fig. 3C), different mutants, including single or double mutants of human RIG-I (h-RIG-I) were generated and co-expressed with empty vector or h-caspase-1. The results showed that the cleaved fragments from all of the mutants were reduced compared to the wild type RIG-I (Supplementary Fig. 3B). We next generated a triple mutant of RIG-I (h-RIG-I-D163/194/234A) and transfected it with caspase-1 in HEK293T cells. Supplementary Fig. 3D revealed that the cleaved band between 25-35 kDa was further weakened, suggesting that the D163, D194 and D234 residues of RIG-I might be the cleavage sites of human derived caspase-1.

To further investigate the effects of RIG-I cleavage on viral replication and type I IFN signaling, Vero cells were transfected with empty vector (EV), RIG-I or co-transfected with caspase-1 and RIG-I, followed by PEDV infection. As shown in Fig. 4E, RIG-I significantly attenuated viral replication, while the co-transfected group reversed this effect. We then generated a RIG-I mutant, RIG-I-D189A, and transfected into IPEC-J2 cells and then infected with PEDV. As expected, wild type RIG-I facilitated *IFN-β* and *ISG15* production and inhibited PEDV replication, and the RIG-I-D189A mutant further enhanced IFN-I signaling and impaired viral

243 replication (Fig. 4F-H). Next, we evaluated the function of RIG-I-1-189aa and
244 RIG-I-190-943aa in activating the innate immune response as well as in viral
245 replication. We found that wild-type RIG-I promoted IFN induction and inhibited
246 PEDV replication, while RIG-I-1-189aa or RIG-I-190-943aa potently reversed IFN-I
247 production and restored viral reproduction (Fig. 4I-K). Taken together, these results
248 collectively demonstrate that caspase-1 targets the D189 residue of porcine RIG-I for
249 cleavage and the cleaved fragments lose their function to inhibit PEDV replication.
250

251 **PLP2 degrades GSDMD-p30 by removing the K27-linked ubiquitin chains at**
252 **K275 residue to inhibit pyroptosis**

253 The activation of caspase-1 can lead to GSDMD cleavage and thus cause pyroptotic
254 cell death. However, according to the above results, PEDV infection did not cause
255 substantial pyroptosis at early stage (Fig. 1H and I). To determine whether PLP2 also
256 targets GSDMD and regulates pyroptosis, HEK293T cells were initially
257 co-transfected with GSDMD-FL and caspase-1 for 6 h, and then PLP2 was transfected
258 in a dose-dependent manner. The immunoblotting results showed that the cleaved
259 fragment of GSDMD (GSDMD-p30) was decreased in the presence of PLP2 (Fig.
260 5A). Meanwhile, we repeatedly observed a reduced protein level of GSDMD-p30
261 after overexpression of PLP2, but had no variation on GSDMD-FL (Fig. 5B and
262 Supplementary Fig. 4A). The LDH release assay and the propidium iodide (PI)
263 staining also confirmed that PLP2 had an inhibitory effect on pyroptotic cell death
264 induced by GSDMD-p30 (Fig. 5C and Supplementary Fig. 4B). As shown in Fig. 5D,

PLP2 had a stronger interaction with GSDMD-p30 than GSDMD-FL, which further demonstrated the complex relationship between GSDMD-p30 and PLP2. In order to evaluate the effect of PLP2 on GSDMD-p30 more directly, we co-transfected GFP-tagged PLP2 and FLAG-tagged GSDMD-p30 in HEK293T cells. GSDMD-p30 was found to localize mainly in the cytoplasm, formed specks and ultimately resulted in rupture of the membrane (Fig. 5E top row). In the presence of PLP2, GSDMD-p30 was evenly dispersed in cytoplasm, failed to form pyroptotic specks (Fig. 5E bottom row). Taken together, we reveal that PLP2 degrades GSDMD-p30 and thus blocks pyroptosis.

To determine which degradation system is responsible for the degradation of GSDMD-p30, we examined the effect of the proteasome inhibitor MG132, the autophagy inhibitor 3MA and CQ on GSDMD-p30 degradation in the presence of PLP2. The results showed that PLP2-mediated degradation of GSDMD-p30 was rescued by MG132, which meant that GSDMD-p30 degradation was corresponded with proteasome pathway (Fig. 6A). We further revealed that all the catalytic mutants of PLP2 (C113A, H272A, D285A) lost the ability to degrade GSDMD-p30 which was also confirmed by the LDH release assay (Fig.6B and C), suggesting that the deubiquitinase activity of PLP2 is essential for the GSDMD-p30 degradation. To determine the lysine residues of GSDMD-p30 to which ubiquitin is attached, we used the UbPred program (http://www.ubpred.org), to predict the potential ubiquitination sites of porcine GSDMD-p30. This analysis revealed three putative lysine residues: K103, K177 and K275. We then generated GSDMD-p30-K103R, K177R and K275R

mutants in which each of these lysine residues was replaced with arginine (R). We co-transfected the wild type porcine GSDMD-p30 and three of its mutants with HA-tagged ubiquitin, followed with immunoblotting. As shown in Fig. 6D, co-transfection of HA-Ub failed to promote GSDMD-p30-K275R mutant ubiquitination, suggesting that Lys275 residue might be the ubiquitination site of GSDMD-p30. Next, we co-transfected HA-tagged ubiquitin mutants (with only one of the seven lysine residues retained as lysine, while the other six replaced with arginine) with GSDMD-p30 in HEK293T cells. The LDH release assay revealed that K27-linked ubiquitin mutant markedly elevated the LDH level (Fig. 6E), which was consistent with our previous study[26]. Ubiquitination assay further confirmed that K27-linked ubiquitin promoted the ubiquitination of GSDMD-p30 (Fig. 6F, lane 2 and 4) and K275R mutant displayed a significant reduction of K27-linked ubiquitination (Fig. 6F, lane 4 and 5). Moreover, we co-expressed the wild type PLP2 or its mutants with HA-tagged K27-linked ubiquitin and FLAG-tagged GSDMD-p30 and then performed Co-IP assay. As expected, wild type PLP2 dramatically reduced K27-linked ubiquitination of GSDMD-p30, while neither of its mutants performed the same effect (Fig. 6G). To further confirm the role of K275 residue of GSDMD, we designed three siRNAs targeting porcine GSDMD. The efficiency of GSDMD knockdown in IPEC-J2 cells was shown in Supplementary Fig. 4C, and we selected si-GSDMD#1 for further studies. IPEC-J2 cells were transfected with GSDMD-FL or GSDMD-FL-K275R upon siRNA-mediated knockdown of GSDMD, followed by PEDV infection. As shown in Supplementary Fig. 4D, GSDMD-FL-K275R facilitated

the viral replication compared to wild type GSDMD-FL, the LDH assay further confirmed this (Supplementary Fig. 4E). Taken together, our results demonstrate that PLP2 is able to degrade GSDMD-p30 by removing the K27-linked ubiquitin chain at K275 residue of GSDMD-p30 and thus abrogate pyroptosis.

CoVs using different strategies to disrupt antiviral response and inhibit pyroptosis

Next, we tested whether papain-like proteases in other genus of CoVs have the same effects on GSDMD-p30 and caspase-1. PEDV-PLP2, SARS-CoV-2-PLpro and PDCoV-PLpro were generated and then transfected into HEK293T cells with GSDMD-p30. As shown in Fig. 7A and B, all these papain-like proteases could inhibit LDH release and degrade GSDMD-p30, which revealed their ability in abrogating pyroptosis. Furthermore, we examined the role of these viral proteins in stabilizing caspase-1 and found that only PEDV PLP2 could promote caspase-1 expression (Fig. 7C). It is possible that PDCoV and SARS-CoV-2 use different ways to activate caspase-1. To evaluate the effect of these viral proteins on PEDV replication, IPEC-J2 cells were transfected with empty vector or these papain-like proteases, and then infected with PEDV. All these papain-like proteases were able to promote viral replication (Fig. 7D). Collectively, GSDMD-p30 was attenuated by papain-like proteases of CoVs, which led to higher viral replication.

It has been reported that the nucleocapsid protein (N) of SARS-CoV-2 activates the NLRP3 inflammasome, thus we hypothesized that NLRP3 inflammasome-mediated

caspase-1 activation could also antagonize IFN production. In that case, we generated THP-1 cell lines stably expressing FLAG-EV-Lentivirus (negative control) or FLAG-N-Lentivirus (Lentivirus carrying the SARS-CoV-2 N gene) (Fig. 7E). Consistent with previous studies[18], FLAG-N-Lentivirus elevated the secretion of IL-1β, suggesting that SARS-CoV-2 N can activate NLRP3 inflammasome (Fig. 7F). To evaluate the role of SARS-CoV-2 N in IFN production, the differentiated macrophages were then stimulated with poly (I:C) and we found that the endogenous RIG-I was significantly reduced in the presence of SARS-CoV-2 N (Fig. 7G). As shown in Fig. 7H and I, the production of IL-1β was elevated while the IFN-β was dramatically reduced by SARS-CoV-2 N. Moreover, qRT-PCR analyses revealed that the expression of *IFN-β* and ISG15 mRNA level were notably repressed by SARS-CoV-2 N (Fig. 7J and K), indicating that the activated caspase-1 targeted RIG-I to abrogate IFN-I signaling. LDH release assay also confirmed the inhibitory effect of SARS-CoV-2 N on GSDMD-mediated pyroptosis (Fig. 7L). Taken together, we unravel a novel antagonistic mechanism employed by different viral proteins from CoVs and thus evade host IFN signaling and pyroptosis (Fig. 8).

Discussion

A variety of viruses have been reported to activate inflammasomes. The inflammasome operates as a platform for caspase-1 activation, resulting in caspase-1-dependent IL-1β release and subsequent pyroptosis. This, in turn, increases the expression of antiviral genes to control invading pathogens[27]. As a countermeasure,

353 viruses have evolved strategies to antagonize host immune response. Previous study
354 has demonstrated that DNA virus-induced inflammasome-mediated active caspase-1
355 cleaves human cGAS at D140 and D157 to dampen IFN production[25]. In the present
356 study, we demonstrated the sophisticated regulation of RNA virus to counteract IFN-I
357 signaling and pyroptosis using active caspase-1 and papain-like protease. We found
358 that CoVs-induced active caspase-1 disrupts IFN-I signaling by cleaving RIG-I to
359 produce inactive fragments. Meanwhile, papain-like protease of CoVs can degrade
360 GSDMD-p30 by removing its K27-linked ubiquitin chain at K275 residue to restrain
361 pyroptosis. Therefore, our work unravels a novel antagonistic mechanism employed
362 by CoVs to evade host antiviral response.

363 To date, most viruses induced caspase-1 activation is mediated by inflammasomes.
364 EV71 3D and ZIKV NS5 activate the NLRP3 inflammasome by interacting with
365 NACHT and the LRR domain of NLRP3[17,28,29]. NS1 of ZIKA also enhances NLRP3
366 inflammasome activation to facilitate its infection[24]. The influenza A virus (IAV)
367 non-structural protein PB1-F2 contributes to severe pathophysiology through
368 triggering NLRP3-dependent caspase-1 activation[30]. Except for NLRP3, viruses can
369 also induce other inflammasomes activation. Human rhinovirus (HRV) 3C protease
370 directly cleaves human NLRP1 between the Glu130 and Gly131 junction, which
371 liberates the activating C-terminal fragment and subsequently promoting NLRP1
372 inflammasome activation[31]. NLRP9b recognizes short double-stranded RNA stretches
373 via RNA helicase Dhx9 and forms inflammasome complexes with ASC and
374 pro-caspase-1 to promote caspase-1-dependent IL-1β release and pyroptosis[32]. Herpes

simplex virus 1 (HSV1) can induce AIM2-, pyrin- and ZBP1-mediated caspase-1 activation, cytokine release and cell death[33]. For coronaviruses, studies have shown that MERS-CoV and at least three different proteins of SARS-CoV-2 can induce NLRP3 inflammasome activation and caspase-1-mediated subsequent pyroptosis[18,20,34,35]. Evidence also demonstrated that circulating monocytes from COVID-19 patients show signs of AIM2 inflammasome activation and caspase-1-meidated GSDMD cleavage and pyroptosis[21]. Unlike the reported manner of caspase-1 activation, our results suggest that PEDV induces porcine caspase-1 activation via its papain-like protease PLP2 through elevating pro-caspase-1 expression by removing its K11-linked ubiquitin chains at K134 residue. Studies have demonstrated that accumulated pro-caspase-1 lead to autoprocessing within the catalytic domain[11-13]. Consequently, active caspase-1 targets to porcine RIG-I for cleavage at D189 residue leading to decreased IFN-I signaling and enhanced PEDV replication. Interestingly, PLPro from SARS-CoV-2 and PDCoV did not use this way to activate caspase-1, as they can trigger NLRP3- or AIM2-mediated caspase-1 activation. Similarly, inflammasome-mediated caspase-1 activation also cleaved human RIG-I to abrogate IFN-I signaling pathway. Therefore, our study suggests that the main purpose of virus-induced inflammasome-mediated caspase-1 activation is to antagonize IFN-I signaling. A newly published study further indicated that SARS-CoV-2 infection induced high expression of pro-caspase-4/11, which may result in its auto-activation in the absence of a ligand[36]. Thus, our results uncover a new and different mechanism of CoVs inducing caspase-1 activation.

Activation of inflammasome is often vital in the host antiviral immune response[35,37-39]. It is obvious that triggering of pyroptosis and inflammasomes activation is detrimental to the replication and survival of viruses. Thus, viruses have also developed strategies to antagonize extensive inflammasome activation and pyroptosis, especially at the early stage of viral infection. The human papillomavirus (HPV) oncoprotein E7 promotes the TRIM21-mediated K33-linked ubiquitination of the IFI16 inflammasome for degradation to inhibit pyroptosis. African swine fever virus (ASFV) pS273R cleaves GSDMD at G107-A108 to generate a shorter N-terminal of GSDMD (GSDMD-N_{1-107}) which is not capable of triggering pyroptosis. The accessory protein (PB1-F2) of H5N1 and H3N2 influenza A viruses (IAV) can bind to the pyrin and LRR domains of NLRP3 and prevent NEK7 binding to stabilize the auto-repressed and closed conformation of NLRP3. 2A and 3C proteases of EV71 can cleave NLRP3 directly to inhibit the activation of inflammasome, while the EV71 3C-like protease can also cleave GSDMD to block the pyroptosis pathway. Our recent research also proved that 3C-like proteases Nsp5 of coronaviruses (PEDV, PDCoV, SARS-CoV-2 and MERS-CoV) can cleave GSDMD at Q193 to produce two fragments that are unable to trigger pyroptosis. SARS-CoV-2 N induces pro-inflammatory cytokines through promoting the assembly and activation of the NLRP3 inflammasome[18]. However, SARS-CoV-2 N protein is also capable of binding to GSDMD directly to inhibit the GSDMD cleavage from caspase-1 to avoid pyroptosis[40]. Our results demonstrated that SARS-CoV-2 N-induced NLRP3 inflammasome activation can antagonize IFN production through cleaving RIG-I by

activated caspase-1. In the present study, we further demonstrated that CoVs (PEDV, PDCoV and SARS-CoV-2) can abrogate pyroptosis by degradation of GSDMD-p30 via their papain-like proteases. Therefore, we discovered a novel mechanism for CoVs to antagonize pyroptosis.

In conclusion, we used PEDV as a model of CoVs to illustrate the sophisticated regulation of CoVs to counteract IFN-I signaling and pyroptosis. For the first time, we demonstrate the role of inflammasome dependent or independent caspase-1 activation in antagonizing IFN-I signaling. Furthermore, we show that papain-like protease of CoVs can inhibit pyroptosis by degradation of GSDMD-p30 through proteasome pathway. Thus, our present study unveils a novel antagonistic mechanism by which CoVs manipulates the cross-talk of IFN signaling and pyroptosis, which might indicate a framework for design of anti-CoVs therapies.

Methods

Reagents and antibodies

Anti-HA (3724) and anti-Caspase-1 (2225) antibodies were purchased from Cell Signaling Technology. Anti-FLAG antibody (F1804), anti-MYC antibody (C3956) and anti-FLAG magnetic beads (10004D) were obtained from Sigma. Anti-FLAG antibody (rabbit source), Goat pAb to MS IgG (Chromeo 546, ab60316), Dnk pAb to Rb IgG (Alexa Fluor 647, ab150075) fluorescent secondary antibodies were acquired from Abcam. Anti-GAPDH antibody, HRP-labeled goat anti-rabbit IgG and goat anti-mouse IgG were from Hangzhou Fudebio. Anti-GSDMDC1 antibody (sc-393581)

was purchased from Santa Cruz. Anti-RIG-I antibody (20566) was obtained from proteintech. The anti-PEDV N monoclonal antibody was prepared in our laboratory as previously described[41]. Efficient eukaryotic transfection reagent VigoFect was obtained from Vigorous Biotechnology (Beijing), Lipo8000TM transfection reagent was obtained from Beyotime Biotechnology while Lipofectamine 2000 transfection reagent was obtained from Invitrogen.

Plasmids

Eukaryotic expression vectors used in this subject were saved in our laboratory. The PLP2 fragment sequence was amplified from cDNA of PEDV strain ZJ15XS0101 (GenBank accession no. KX55SO0281) which was isolated by our collaborating laboratories for generational preservation, while amplification of the porcine GSDMD gene and the porcine caspase-1 gene used cDNA of IPEC-J2 as a templet. The PLP2 gene was cloned to PRK-MYC vector, and the porcine GSDMD gene was cloned onto p3×FLAG-CMV vector. The porcine caspase-1 gene was cloned to PCMV-HA and p3×FLAG-CMV vector, respectively. Porcine GSDMD-p30 fragment was amplified from the p3×FLAG-N-GSDMD-FL plasmid and cloned onto p3×FLAG-CMV. PLP2, caspase-1 and GSDMD-p30 enzyme active site mutants were constructed based on the eukaryotic expression plasmids PRK-MYC-PEDV-PLP2, HA-PCMV-Caspase-1 and p3×FLAG-GSDMD-p30. The plasmids encoding SARS-CoV-2 PLPro, PDCoV PLPro and SARS-CoV-2-N were synthesized by Tsingke Biotech. Primers used in the plasmids construction are listed in table 1 in supplementary materials.

Cell culture and transfection

IPEC-J2 cells, Vero cells and HEK293T cells were cultured in Dulbecco's modified Eagle's medium (DMEM) with added 10% FBS and 1% penicillin-streptomycin. Wild type THP-1 and caspase-1 deficient THP-1 were cultured in PRIM 1640 medium containing 10% FBS and 1% penicillin-streptomycin solution. The PEDV strain ZJ15XS0101 (GenBank accession no. KX55SO0281) was isolated and stored in our laboratory[42]. When HEK293T cells seeded in plates grow to about a density of 60%~80%, indicated plasmids were transfected to the cells by VigoFect according to the manufacturer's operation guide. When IPEC-J2 and Vero seeded in plates grow to approximately 70%~80%, they were transfected with corresponding plasmids using Lipo8000 transfection reagent according to the manufacturer's introduction. Lipo2000 was applied in the transfection of poly(I:C) (Merck) to IPEC-J2 during the second transfection period.

Viral infection

Viral infection was performed when the IPEC-J2 or Vero cells grow to the density around 80%~90% or after the transfection of other indicated plasmids.

Lentivirus infection

SARS-COV-2-N over-expressing THP-1 cells were generated using lentiviral infection technique. After cloning *SARS-COV-2-N* coding sequence to the pLVX-IRES-Puro-3×Flag lentiviral vector plasmid, HEK293T cells were co-transfected with pLVX-IRES-Puro-3×Flag-SARS-COV-2-N, pMD2G and PSPAX2. Supernatant was collected after 48 h incubation for further lentiviral concentration.

485 **Inhibitors treatment**

486 The caspase-1 specific inhibitor VX765 diluted to 20 μM was used after plasmid
487 transfection, during viral infection or before poly(I:C) transfection. Protein synthesis
488 inhibitor cycloheximide (CHX) diluted to 25 μg/ml was added at different time points
489 before receiving samples. Fresh culture medium containing proteasome inhibitor
490 MG132, autophagy initiation inhibitor 3MA or autophagy lysosome inhibitor CQ of
491 appropriate concentration were added to different wells of cell-culturing plates 6 h
492 before receiving samples.

493 **Cytotoxicity assay**

494 Cells transfected with corresponding plasmids for 24 h were applied to cytotoxicity
495 test using CytoTox 96® Reagent (Promega) according to the manufacturer's manual.
496 OD values were read at 492 nm on an enzyme marker (Thermo Scientific).

497 **Immunoblotting**

498 Total proteins were extracted from cells lysed by RIPA lysis buffer (Beyotime
499 Biotechnology) supplemented with 1% Phenylmethanesulfonyl fluoride (PMSF)
500 (Beyotime Biotechnology). After being separated on the 10% SDS-PAGE gel (Verde
501 Biotechnology), protein stripes were transferred onto the polyvinylidene difluoride
502 (PVDF) membranes (Bio-rad). Membranes were blocked in the blocking buffer
503 (Beyotime Biotechnology), followed by incubation with primary antibodies and
504 positioning with secondary antibodies. Chemiluminescent signals were captured by an
505 ECL chemiluminescence imaging analysis system (Clinx Science Instruments).

506

Co-immunoprecipitation

Cells were lysed using IP lysis buffer (Beyotime Biotechnology) for 15 min at 4℃, and then centrifuged at speed 10000 rpm at 4℃ for 15 min. After being incubated with the supernatant of the cell lysis solution in a flip mixer (Kylin-Bell) overnight, the magnetic beads coated with FLAG-antibodies (sigma) were washed with coIP-buffer for 5 times. Soaking in 1×loading buffer, magnetic beads absorbed with target proteins were denatured for 10 min in a boiling water bath. After discarding magnetic beads, the remaining protein samples were applied to subsequent immunoblotting assay.

Confocal immunofluorescence assay

HEK293T cells were seeded on glass slides placed in 24-well plates. After being transfected for 24 h, cells were fixed with Immunol Staining Fix Solution (Beyotime), permeabilized with Immunostaining Permeabilization Solution with Saponin (Beyotime), blocked with QuickBlock Blocking Buffer for Immunol Staining (Beyotime), and then incubated with indicated antibodies. The cells were observed under a laser confocal microscope (Olympus).

ELISA

Supernatants collected from transfected cells were applied to the detection of IL-1β and IFN-β according to the manufacturer's instructions. Each trial group was conducted independently for three times.

Total RNA extraction and reverse transcription

Add RNA-easy Isolation Reagent (Vazyme Biotechnology) to cells to gather lysis

529 solution containing cells. Follow the manufacturer's introduction to extract the RNA.
530 After measuring the product RNA concentration, use the HiScript III RT SuperMix for
531 qPCR (+gDNA wiper) (Vazyme Biotechnology) to reverse transcribe RNA to cDNA.

532 **Quantitative real-time polymerase chain reaction (qRT-PCR)**

533 qRT-PCR was performed with ChamQ Universal SYBR qPCR Master Mix (Vazyme
534 Biotechnology) according to the manufacturer's requirements. Primers demanded in
535 this analysis were listed in table 2 in supplementary materials.

536 **RNA interference**

537 SiRNAs (Genepharma) specific for porcine GSDMD were transfected into IPEC-J2
538 cells using the Lipofectamine 8000 transfection reagent according to the
539 manufacturer's instructions. The sequences of GSDMD siRNAs were listed in table 3
540 in supplementary materials.

541 **Propidium iodide staining**

542 Cells were incubated with Propidium iodide (PI) (BD Bioscience) for 15 min under
543 light-proof conditions after transfection with indicated plasmids for 24 h. Dyeing
544 condition was observed under fluorescence microscope (Nikon).

545 **Statistical analysis**

546 All experiments were performed independently at least three times. Data were
547 presented as the mean ± standard deviation (SD), analyzed and used for statistical
548 graphing by GraphPad Prism 8, the significance of differences was determined by
549 One-way ANOVA or Student's *t*-test. The significance of differences ranked as:
550 ****stands for P<0.0001, ***stands for P<0.001, ** stands for P<0.01, * stands for

551 P<0.05 and ns stands for non-significant difference.

552 **Data availability**

553 The authors declare that all data supporting the findings of this article are available
554 within the paper and the supplementary information files or are available from the
555 authors upon request.

556

557 # References

558 1. Zhang, Q. & Yoo, D. Immune evasion of porcine enteric coronaviruses and viral
559 modulation of antiviral innate signaling. *Virus Res* **226**, 128-141 (2016).
560 2. Stevenson, G.W. *et al.* Emergence of Porcine epidemic diarrhea virus in the United States:
561 clinical signs, lesions, and viral genomic sequences. *J Vet Diagn Invest* **25**, 649-654
562 (2013).
563 3. Jung, K. & Saif, L.J. Porcine epidemic diarrhea virus infection: Etiology, epidemiology,
564 pathogenesis and immunoprophylaxis. *Vet J* **204**, 134-143 (2015).
565 4. Xing, Y. *et al.* The papain-like protease of porcine epidemic diarrhea virus negatively
566 regulates type I interferon pathway by acting as a viral deubiquitinase. *J Gen Virol* **94**,
567 1554-1567 (2013).
568 5. Chu, H.F. *et al.* Structural and Biochemical Characterization of Porcine Epidemic Diarrhea
569 Virus Papain-Like Protease 2. *J Virol* **96**, e0137221 (2022).
570 6. Clementz, M.A. *et al.* Deubiquitinating and interferon antagonism activities of
571 coronavirus papain-like proteases. *J Virol* **84**, 4619-4629 (2010).
572 7. Zheng, D., Chen, G., Guo, B., Cheng, G. & Tang, H. PLP2, a potent deubiquitinase from
573 murine hepatitis virus, strongly inhibits cellular type I interferon production. *Cell Res* **18**,
574 1105-1113 (2008).
575 8. Wang, Y. *et al.* Porcine transmissible gastroenteritis virus inhibits NF-kappaB activity via
576 nonstructural protein 3 to evade host immune system. *Virol J* **16**, 97 (2019).
577 9. Man, S.M. & Kanneganti, T.D. Converging roles of caspases in inflammasome activation,
578 cell death and innate immunity. *Nat Rev Immunol* **16**, 7-21 (2016).
579 10. Ball, D.P. *et al.* Caspase-1 interdomain linker cleavage is required for pyroptosis. *Life Sci*
580 *Alliance* **3** (2020).
581 11. Boucher, D. *et al.* Caspase-1 self-cleavage is an intrinsic mechanism to terminate
582 inflammasome activity. *J Exp Med* **215**, 827-840 (2018).
583 12. Ross, C. *et al.* Inflammatory Caspases: Toward a Unified Model for Caspase Activation by
584 Inflammasomes. *Annu Rev Immunol* **40**, 249-269 (2022).
585 13. Bambouskova, M. *et al.* Itaconate confers tolerance to late NLRP3 inflammasome
586 activation. *Cell Rep* **34**, 108756 (2021).
587 14. Jorgensen, I. & Miao, E.A. Pyroptotic cell death defends against intracellular pathogens.
588 *Immunol Rev* **265**, 130-142 (2015).

15. Liu, X. *et al.* Inflammasome-activated gasdermin D causes pyroptosis by forming membrane pores. *Nature* **535**, 153-158 (2016).
16. Sborgi, L. *et al.* GSDMD membrane pore formation constitutes the mechanism of pyroptotic cell death. *EMBO J* **35**, 1766-1778 (2016).
17. Wang, W. *et al.* Zika virus infection induces host inflammatory responses by facilitating NLRP3 inflammasome assembly and interleukin-1beta secretion. *Nat Commun* **9**, 106 (2018).
18. Pan, P. *et al.* SARS-CoV-2 N protein promotes NLRP3 inflammasome activation to induce hyperinflammation. *Nat Commun* **12**, 4664 (2021).
19. Ahn, M. *et al.* Dampened NLRP3-mediated inflammation in bats and implications for a special viral reservoir host. *Nat Microbiol* **4**, 789-799 (2019).
20. Jiang, Y. *et al.* Complement Receptor C5aR1 Inhibition Reduces Pyroptosis in hDPP4-Transgenic Mice Infected with MERS-CoV. *Viruses* **11** (2019).
21. Junqueira, C. *et al.* SARS-CoV-2 infects blood monocytes to activate NLRP3 and AIM2 inflammasomes, pyroptosis and cytokine release. *Res Sq* (2021).
22. Tsu, B.V. *et al.* Diverse viral proteases activate the NLRP1 inflammasome. *Elife* **10** (2021).
23. Shi, F. *et al.* Coronaviruses Nsp5 Antagonizes Porcine Gasdermin D-Mediated Pyroptosis by Cleaving Pore-Forming p30 Fragment. *mBio*, e0273921 (2022).
24. Zheng, Y. *et al.* Zika virus elicits inflammation to evade antiviral response by cleaving cGAS via NS1-caspase-1 axis. *EMBO J* **37** (2018).
25. Wang, Y. *et al.* Inflammasome Activation Triggers Caspase-1-Mediated Cleavage of cGAS to Regulate Responses to DNA Virus Infection. *Immunity* **46**, 393-404 (2017).
26. Shi, Y. *et al.* E3 ubiquitin ligase SYVN1 is a key positive regulator for GSDMD-mediated pyroptosis. *Cell Death Dis* **13**, 106 (2022).
27. Shrivastava, G., Leon-Juarez, M., Garcia-Cordero, J., Meza-Sanchez, D.E. & Cedillo-Barron, L. Inflammasomes and its importance in viral infections. *Immunol Res* **64**, 1101-1117 (2016).
28. Wang, W. *et al.* EV71 3D Protein Binds with NLRP3 and Enhances the Assembly of Inflammasome Complex. *PLoS Pathog* **13**, e1006123 (2017).
29. He, Z. *et al.* NLRP3 Inflammasome Activation Mediates Zika Virus-Associated Inflammation. *J Infect Dis* **217**, 1942-1951 (2018).
30. McAuley, J.L. *et al.* Activation of the NLRP3 inflammasome by IAV virulence protein PB1-F2 contributes to severe pathophysiology and disease. *PLoS Pathog* **9**, e1003392 (2013).
31. Robinson, K.S. *et al.* Enteroviral 3C protease activates the human NLRP1 inflammasome in airway epithelia. *Science* **370** (2020).
32. Zhu, S. *et al.* Nlrp9b inflammasome restricts rotavirus infection in intestinal epithelial cells. *Nature* **546**, 667-670 (2017).
33. Lee, S. *et al.* AIM2 forms a complex with pyrin and ZBP1 to drive PANoptosis and host defence. *Nature* **597**, 415-419 (2021).
34. Sun, X. *et al.* SARS-CoV-2 non-structural protein 6 triggers NLRP3-dependent pyroptosis by targeting ATP6AP1. *Cell Death Differ* **29**, 1240-1254 (2022).
35. Lee, S., Channappanavar, R. & Kanneganti, T.D. Coronaviruses: Innate Immunity, Inflammasome Activation, Inflammatory Cell Death, and Cytokines. *Trends Immunol* **41**,

1083-1099 (2020).

36. Eltobgy, M.M. *et al.* Caspase-4/11 exacerbates disease severity in SARS-CoV-2 infection by promoting inflammation and immunothrombosis. *Proc Natl Acad Sci U S A* **119**, e2202012119 (2022).

37. Kanneganti, T.D. *et al.* Bacterial RNA and small antiviral compounds activate caspase-1 through cryopyrin/Nalp3. *Nature* **440**, 233-236 (2006).

38. Kanneganti, T.D. *et al.* Critical role for Cryopyrin/Nalp3 in activation of caspase-1 in response to viral infection and double-stranded RNA. *J Biol Chem* **281**, 36560-36568 (2006).

39. Thomas, P.G. *et al.* The intracellular sensor NLRP3 mediates key innate and healing responses to influenza A virus via the regulation of caspase-1. *Immunity* **30**, 566-575 (2009).

40. Ma, J. *et al.* SARS-CoV-2 nucleocapsid suppresses host pyroptosis by blocking Gasdermin D cleavage. *EMBO J* **40**, e108249 (2021).

41. Shan, Y. *et al.* Nucleocapsid protein from porcine epidemic diarrhea virus isolates can antagonize interferon-lambda production by blocking the nuclear factor-kappaB nuclear translocation. *J Zhejiang Univ Sci B* **19**, 570-580 (2018).

42. Zhou, Y. *et al.* Effect of route of inoculation on innate and adaptive immune responses to porcine epidemic diarrhea virus infection in suckling pigs. *Vet Microbiol* **228**, 83-92 (2019).

Acknowledgements

This work was financially supported by the National Natural Science Foundation of China (32072817), the Zhejiang Provincial Key R&D Program of China (2021C02049 and 2021C02050), the “Pioneer” and “Leading Goose” R&D Program of Zhejiang Province (2022C02031), High-level Talents Special Support Plan of Zhejiang Province (2021R52041), the Agricultural Major Technology Synergy Extension Project of Zhejiang Province (2021XTTGXM02-05), the Scientific Research Fund of Zhejiang Provincial Education Department (Y202045613, Y202148324) and the Zhejiang Provincial Natural Science Foundation of China (LY18C180001, LY21C180001).

We thank Dr. Ying Shan in the Shared Experimental Platform for Core Instruments,

College of Animal Sciences, Zhejiang University for assistance with analysis of laser confocal microscopy imaging.

Author contributions

X.F., Y.Y., W.X. and F.S. contributed to the design of experiments and performed most of the experiments. D.L, X.L., N.C., Q.L. and Y.S. performed some experiments. X.F, D.L., W.X., X.L. and F.S. contributed to data analysis. X.F., D.L., Y.Y. and F.S. contributed to writing the manuscript.

Competing interests

The authors declare no competing interests.

Figure legends

Figure 1. PEDV infection elevates the expression of caspase-1. A The intestinal tissue lysates were extracted from healthy or PEDV naturally-infected piglets for immunoblotting (IB). **B, C** IPEC-J2 cells were mock infected or infected with PEDV at an MOI of 0.5, followed by cycloheximide (CHX) treatment (25 μg/ml) for 6 h. The indicated gene mRNA was quantified by qRT-PCR (**B**). The indicated proteins were analyzed by immunoblotting (**C**). **D** Vero cells were transfected with plasmid encoding porcine caspase-1. At 24 h after transfection, the cells were mock infected or infected with different doses of PEDV for another 24 h, the cell lysates were then processed for immunoblotting. **E** Vero cells were transfected with plasmid encoding porcine caspase-1. At 24 h after transfection, the cells were mock infected or infected with PEDV at an MOI of 0.1. At indicated time points after infection, the cell lysates were analyzed by immunoblotting. **F, H** Vero cells were co-transfected with plasmids encoding GSDMD-FL and caspase-1. At 12 h after transfection, the cells were mock infected or infected with different doses of PEDV for another 24 h, the cell lysates were processed for immunoblotting (**F**), the supernatants were collected for LDH release assay (**H**). **G, I** Vero cells were co-transfected with plasmids encoding GSDMD-FL and caspase-1. At 12 h after transfection, the cells were mock infected or infected with PEDV at an MOI of 0.05. At indicated time points after infection, the cell lysates were analyzed by immunoblotting (**G**), the supernatants were collected for LDH release assay (**I**). All results shown are representative of at least three independent experiments. ****stands for P<0.0001, ***stands for P<0.001, ** stands

698 for P<0.01, * stands for P<0.05 and ns stands for non-significant difference.

699

700 **Figure 2. PLP2 inhibits the proteasomal degradation of caspase-1 by removing**
701 **K11-linked ubiquitin chains at Lys134. A** HEK293T cells were co-transfected with
702 HA-caspase-1-C285A and increasing amount of MYC-PEDV-PLP2. Cell lysates were
703 analyzed by immunoblotting. **B** HEK293T cells were co-transfected with
704 HA-caspase-1-C285A together with empty vector or MYC-PEDV-PLP2 then treated
705 with cycloheximide (CHX) (25 μg/ml) for the indicated time points. Cell lysates were
706 analyzed by immunoblotting. **C** HEK293T cells were co-transfected with
707 HA-caspase-1-C285A together with wild-type PEDV PLP2 or its protease-defective
708 mutants (C113A, H272A and D285A). Cell lysates were analyzed by immunoblotting.
709 **D** Immunoprecipitation analysis of HEK293T cells expressing FLAG-caspase-1 and
710 HA-UB together with MYC-tagged empty vector, wild-type PEDV-PLP2 or its
711 mutants as indicated. Anti-FLAG immunoprecipitates were analyzed by
712 immunoblotting (IP). The expression levels of the transfected proteins were analyzed
713 by immunoblotting (INPUT). **E** HEK293T cells were co-transfected with
714 FLAG-caspase-1 or its mutant FLAG-caspase-1-K134R together with increasing
715 amount of HA-tagged K11-linked ubiquitin (HA-K11). Cell lysates were analyzed by
716 immunoblotting. **F** HEK293T cells were transfected with FLAG-caspase-1 together
717 with HA-K11 and MYC-PEDV-PLP2 as indicated. Cell lysates were analyzed by
718 immunoblotting. **G** HEK293T cells were transfected with HA-caspase-1-C285A or its
719 mutant HA-caspase-1-C285A-K134R together with MYC-tagged empty vector or

PEDV PLP2. Cell lysates were analyzed by immunoblotting. **H** Vero cells were transfected with FLAG-caspase-1 together with HA-K11 or empty vector. At 24 h after transfection, the cells were mock infected or infected with PEDV at an MOI of 0.05 for another 24 h. Immunoprecipitation was performed with anti-FLAG binding beads and analyzed by immunoblotting. All results shown are representative of at least three independent experiments.

Figure 3. Caspase-1 attenuates IFN-I signaling during PEDV infection. A-D Relative qRT-PCR analysis of *IFN-α*, *IFN-β*, *ISG15* and *OAS1* mRNA levels in IPEC-J2 cells transfected with empty vector or caspase-1 for 24 h, and then stimulated with poly (I:C) (200 ng/ml) for another 12 h. **E, F** Relative qRT-PCR analysis of *IFN-β* and *ISG15* mRNA levels in IPEC-J2 cells treated with VX765 (20 μM) or DMSO, followed by poly (I:C) (200 ng/ml) transfection for 12 h. **G, H** Relative qRT-PCR analysis of *IFN-β* and *ISG15* mRNA levels in wild type (WT) or caspase-1 knockout (KO) THP-1 cells transfected with poly (I:C) (200 ng/ml) for 12 h. **I, J** Relative qRT-PCR analysis of *IFN-β* and *ISG15* mRNA levels in IPEC-J2 cells transfected with empty vector or PEDV PLP2 for 24 h, followed with poly (I:C) (200 ng/ml) transfection for another 12 h. **K, L** Relative qRT-PCR analysis of *IFN-β* and *ISG15* mRNA levels in IPEC-J2 cells transfected with empty vector or caspase-1 for 24 h, followed with PEDV infection (MOI=0.5) for another 24 h. **M, N** Relative qRT-PCR analysis of *IFN-β* and *ISG15* mRNA levels in IPEC-J2 cells treated with VX765 (20 μM) or DMSO, followed with PEDV infection (MOI=0.5) for 24 h. **O, P**

742 Relative qRT-PCR analysis of *IFN-β* and *ISG15* mRNA levels in IPEC-J2 cells
743 transfected with empty vector or PEDV PLP2 for 24 h, followed with PEDV infection
744 (MOI=0.5) for another 24 h. **Q** IPEC-J2 cells were transfected with empty vector or
745 PEDV PLP2 for 24 h, followed with PEDV infection at an MOI of 0.5 for another 24
746 h. The indicated gene mRNA levels were quantified by qRT-PCR and the indicated
747 proteins were analyzed by immunoblotting. **R** Relative qRT-PCR analysis of *PEDV S*
748 mRNA levels in IPEC-J2 cells transfected with empty vector or increasing amount of
749 caspase-1 for 12 h, followed with PEDV infection (MOI=0.1) for another 24 h. **S**
750 Relative qRT-PCR analysis of *PEDV S* mRNA levels in IPEC-J2 cells transfected
751 with empty vector and treated with or without VX765 (20 μM), co-treated with
752 necrosulfonamide (NSA 8 μM), followed with PEDV infection (MOI=0.1) for another
753 24 h. All results shown are representative of at least three independent experiments.
754 ****stands for P<0.0001, ***stands for P<0.001, ** stands for P<0.01, * stands for
755 P<0.05 and ns stands for non-significant difference.
756
757 **Figure 4. Cleavage of RIG-I by caspase-1 ensures PEDV replication. A** HEK293T
758 cells co-transfected with FLAG-caspase-1 and S-MYC-RIG-I (porcine derived) were
759 lysed and immunoprecipitated with anti-FLAG beads and analyzed by
760 immunoblotting. **B, C** HEK293T cells were co-transfected with S-MYC-RIG-I and
761 increasing amount of HA-caspase-1 or HA-caspase-1-C285A. Cell lysates were
762 analyzed by immunoblotting. **D** HEK293T cells were co-transfected with wild-type
763 (WT) S-MYC-RIG-I or its mutants (D163A, D189A, D194A, D199/202/203A,

D209A) together with empty vector or HA-caspase-1. Cell lysates were analyzed by immunoblotting. **E** Vero cells were transfected with empty vector, RIG-I together with or without caspase-1. At 12 h after transfection, the cells were mock infected or infected with PEDV at an MOI of 0.05. The indicated gene mRNA levels were quantified by qRT-PCR. **F-H** Relative qRT-PCR analysis of *PEDV S, IFN-β* and *ISG15* mRNA levels in IPEC-J2 cells transfected with empty vector, RIG-I or RIG-I-D189A for 24 h, followed by PEDV infection (MOI=0.5) for another 24 h. **I-K** Relative qRT-PCR analysis of *PEDV S, IFN-β* and *ISG15* mRNA levels in IPEC-J2 cells transfected with empty vector, RIG-I, RIG-I-1-189aa or RIG-I-190-943aa for 24 h, followed by PEDV infection (MOI=0.5) for another 24 h. All results shown are representative of at least three independent experiments. ****stands for P<0.0001, ***stands for P<0.001, ** stands for P<0.01, * stands for P<0.05 and ns stands for non-significant difference.

Figure 5. PLP2 degrades GSDMD-p30 to inhibit pyroptosis. A HEK293T cells were initially co-transfected with FLAG-GSDMD-FL and HA-caspase-1. At 6 h after transfection, the cells were transfected with increasing amount of MYC-PEDV-PLP2. Cell lysates were analyzed by immunoblotting. **B, C** HEK293T cells were co-transfected with FLAG-GSDMD-p30 and increasing amount of MYC-PEDV-PLP2. Cell lysates were analyzed by immunoblotting (**B**). The supernatants were collected for LDH release assay (**C**). **D** HEK293T cells co-transfected with MYC-PEDV-PLP2 together with empty vector,

FLAG-GSDMD-FL or FLAG-GSDMD-p30 were lysed and immunoprecipitated with anti-FLAG beads and analyzed by immunoblotting. **E** HEK293T cells were transfected with FLAG-GSDMD-p30 and GFP-PLP2 respectively or together for 24 h, and then FLAG-GSDMD-p30 cells were labeled with indicated antibodies. Subcellular localization of FLAG-GSDMD-p30 (red), GFP-PLP2 (green), and DAPI (blue, nucleus marker) were visualized with confocal microscopy. All results shown are representative of at least three independent experiments. ****stands for P<0.0001, ***stands for P<0.001, ** stands for P<0.01, * stands for P<0.05 and ns stands for non-significant difference.

Figure 6. PLP2 removes the K27-linked ubiquitin chain at K275 residue of GSDMD-p30. A HEK293T cells were transfected with FLAG-GSDMD-p30 together with empty vector or MYC-PEDV-PLP2 then treated with DMSO, MG132 (10 μM), 3MA (1 mM) or CQ (40 μM) for 6 h. Cell lysates were analyzed by immunoblotting. **B, C** HEK293T cells were co-transfected with FLAG-GSDMD-p30 together with empty vector, wild type PLP2 or its protease-defective mutants (C113A, H272A, D285A). The supernatants were collected for LDH release assay (**B**). Cell lysates were analyzed by immunoblotting (**C**). **D** HEK293T cells were co-expressed with FLAG-GSDMD-p30 or its mutants (K103R, K177R, K275R) together with empty vector or HA-UB. Cell lysates were analyzed by immunoblotting. **E** HEK293T cells were co-transfected with FLAG-GSDMD-p30 and HA-tagged WT ubiquitin or its mutants (K6, K11, K27, K29, K33, K48, K63, KO). The supernatants were collected

for LDH release assay. **F** Co-immunoprecipitation and immunoblot analysis of extracts of HEK293T cells transfected with FLAG-GSDMD-p30 or FLAG-GSDMD-p30-K275R together with HA-UB or HA-K27 ubiquitin. **G** Co-immunoprecipitation and immunoblot analysis of extracts of HEK293T cells transfected with FLAG-GSDMD-p30 and HA-K27 ubiquitin together with empty vector, wild type PLP2 or its mutants (C113A, H272A, D285A). All results shown are representative of at least three independent experiments. ****stands for P<0.0001, ***stands for P<0.001, ** stands for P<0.01, * stands for P<0.05 and ns stands for non-significant difference.

Figure 7. Papain-like proteases in other CoVs can also abrogate pyroptosis by degradation of GSDMD-p30. A, B HEK293T cells were transfected with FLAG-GSDMD-p30 together with empty vector, PEDV-PLP2, SARS-CoV-2-PLPro or PDCoV-PLPro. The supernatants were collected for LDH release assay (**A**). Cell lysates were analyzed by immunoblotting (**B**). **C** HEK293T cells were transfected with HA-caspase-1-C285A together with empty vector, PEDV-PLP2, SARS-CoV-2-PLPro or PDCoV-PLPro. Cell lysates were analyzed by immunoblotting. **D** IPEC-J2 cells were transfected with empty vector, PEDV-PLP2, SARS-CoV-2-PLPro or PDCoV-PLPro. At 24 h after transfection, the cells were infected with PEDV at an MOI of 0.1 for another 24 h. The indicated gene mRNA levels were quantified by qRT-PCR (top). Cell lysates were analyzed by immunoblotting (bottom). **E** Immunoblot analysis of extracts of THP-1 cells stably

infected with FLAG-EV-Lentivirus or FLAG-N-Lentivirus. **F** PMA-differentiated THP-1 macrophages were stably infected with FLAG-EV-Lentivirus or FLAG-N-Lentivirus. The supernatants were collected and analyzed by ELISA for IL-1β. **G-L** PMA-differentiated THP-1 macrophages were stably infected with FLAG-EV-Lentivirus or FLAG-N-Lentivirus, followed with poly (I:C) (200 ng/ml) transfection for 6 h. Cell lysates were analyzed by immunoblotting (**G**). The supernatants were collected and analyzed by ELISA for IL-1β (**H**), IFN-β (**I**) and for LDH release assay (**L**). The mRNA levels of *IFN-β* (**J**) and *ISG15* (**K**) were quantified by qRT-PCR. All results shown are representative of at least three independent experiments. ****stands for P<0.0001, ***stands for P<0.001, ** stands for P<0.01, * stands for P<0.05 and ns stands for non-significant difference.

Figure 8. Mechanistic diagram of CoVs antagonizing antiviral responses and pyroptosis.

Supplementary Fig. 1. PEDV PLP2 interacts with both caspase-1 and GSDMD. A Vero cells were transfected with FLAG-GSDMD-FL and then infected with PEDV at an MOI of 0.05. Immunoprecipitation was performed with anti-FLAG antibody. The potential GSDMD-binding viral proteins were evaluated using MS analysis. **B** Co-immunoprecipitation and immunoblot analysis of extracts of HEK293T cells transfected with MYC-PEDV-PLP2 together with FLAG-GSDMD-FL or FLAG-tagged empty vector. **C** Co-immunoprecipitation and immunoblot analysis of

852 extracts of HEK293T cells transfected with MYC-PEDV-PLP2 together with
853 FLAG-caspase-1 or FLAG-tagged empty vector, then treated with VX765 (20 μM). **D**
854 HEK293T cells were transfected with FLAG-GSDMD-FL, GFP-PLP2 and
855 HA-caspase-1 respectively or together for 24 h, and then the cells were labeled with
856 indicated antibodies. Subcellular localization of FLAG-GSDMD-FL (cyan),
857 GFP-PLP2 (green), HA-caspase-1 (red) and DAPI (blue, nucleus marker) were
858 visualized with confocal microscopy. All results shown are representative of at least
859 three independent experiments.
860
861 **Supplementary Fig. 2. The papain-like protease 2 of PEDV inhibits proteasomal**
862 **degradation of caspase-1. A** HEK293T cells were transfected with
863 FLAG-GSDMD-FL and HA-caspase-1 together with increasing amount of
864 MYC-PEDV-PLP2. Cell lysates were analyzed by immunoblotting. **B** HEK293T cells
865 were co-transfected with FLAG-GSDMD-FL together with empty vector or
866 MYC-PEDV-PLP2 then treated with cycloheximide (CHX) (25 μg/ml) for the
867 indicated time points. Cell lysates were analyzed by immunoblotting. **C**
868 Co-immunoprecipitation and immunoblot analysis of extracts of HEK293T cells
869 transfected with FLAG-caspase-1 or FLAG-caspase-1-K134R together with HA-K11
870 ubiquitin. All results shown are representative of at least three independent
871 experiments.
872
873 **Supplementary Fig. 3. RIG-I was cleaved by caspase-1. A** (long exposure of Fig.

4D) HEK293T cells were co-transfected with wild-type (WT) S-MYC-RIG-I or its mutants (D163A, D189A, D194A, D199/202/203A, D209A) together with empty vector or HA-caspase-1. Cell lysates were analyzed by immunoblotting. **B** HEK293T cells were co-transfected with wild-type (WT) h-FLAG-RIG-I or its single, double mutants (D163A, D194A, D234A, D163/194A, D163/234A, D194/234A) together with empty vector or H-HA-caspase-1. Cell lysates were analyzed by immunoblotting. **C** Alignment of the amino acid sequence of RIG-Is from different species. **D** HEK293T cells were co-transfected with wild-type (WT) h-FLAG-RIG-I or its triple mutant (D163/194/234A) together with empty vector or h-HA-caspase-1. Cell lysates were analyzed by immunoblotting.

Supplementary Fig. 4. PLP2 degrades GSDMD-p30 by removing the K27-linked ubiquitin chains at K275 residue to inhibit pyroptosis. A HEK293T cells were transfected with FLAG-GSDMD-FL together with increasing amount of MYC-PEDV-PLP2. Cell lysates were analyzed by immunoblotting. **B** HEK293T cells were co-transfected with FLAG-GSDMD-p30 and MYC-PEDV-PLP2, then the cells were performed with propidium iodide (PI) staining analysis. **C** Immunoblot analysis of extracts of IPEC-J2 cells transfected with negative control (NC) siRNA or GSDMD siRNA (si-GSDMD#1, si-GSDMD#2, si-GSDMD#3). Cell lysates were analyzed by immunoblotting. **D, E** IPEC-J2 cells were transfected with GSDMD siRNA (si-GSDMD#1) for 24 h and then expressed with GSDMD-FL or GSDMD-FL-K275R for another 24 h. The cells were then infected with PEDV at an MOI of 0.1 for 24 h.

The indicated gene mRNA levels were quantified by qRT-PCR (**D**). The supernatants were collected for LDH release assay (**E**). All results shown are representative of at least three independent experiments. ****stands for P<0.0001, ***stands for P<0.001, ** stands for P<0.01, * stands for P<0.05 and ns stands for non-significant difference.

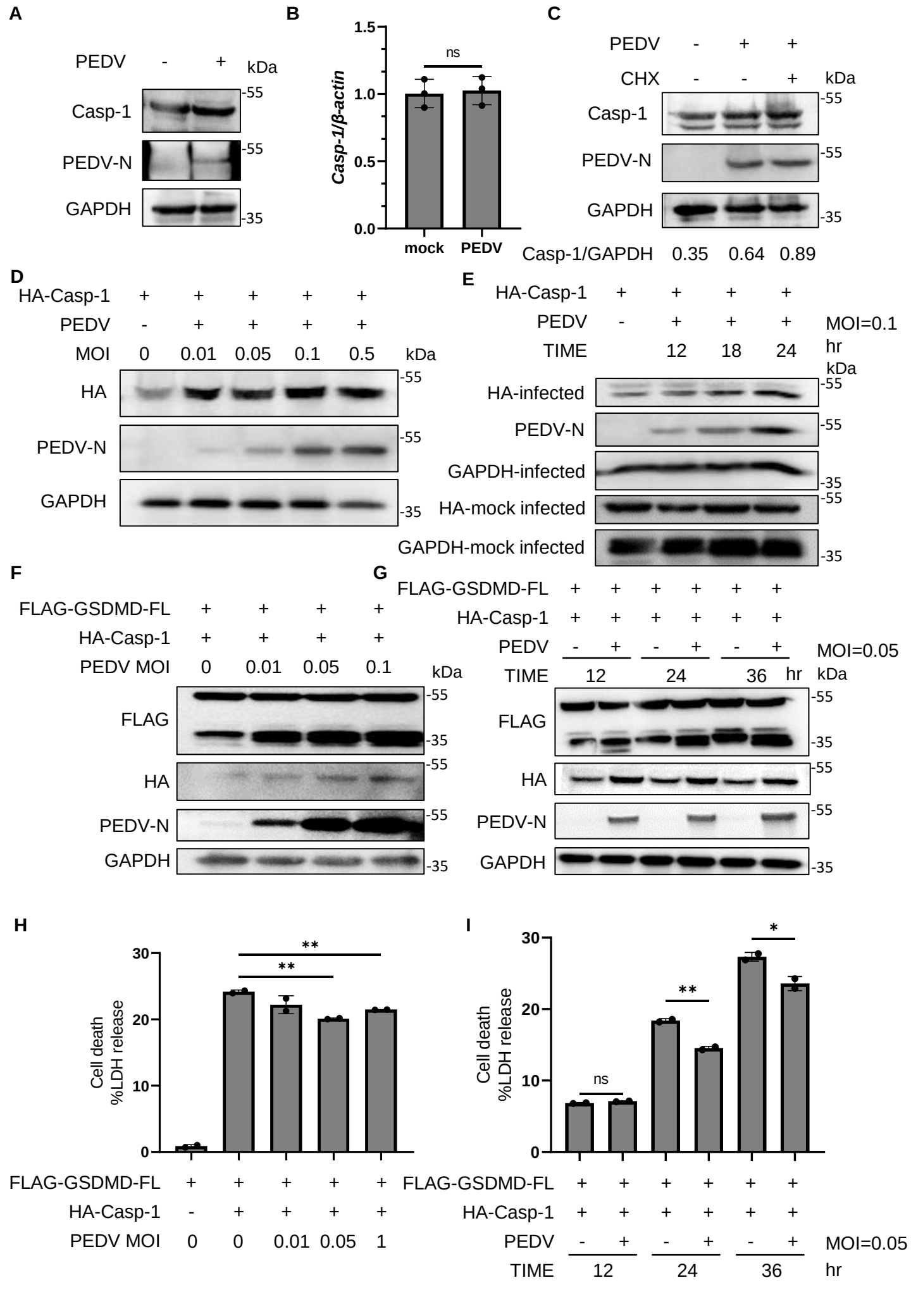
A
PEDV - +
kDa
Casp-1
PEDV-N
GAPDH
-55
-55
-35
B
Casp-1/β-actin
1.5
1.0
0.5
0.0
ns
mock
PEDV
C
PEDV - + +
CHX - - +
kDa
Casp-1
PEDV-N
GAPDH
-55
-55
-35
Casp-1/GAPDH 0.35 0.64 0.89
D
HA-Casp-1 + + + + +
PEDV - + + + +
MOI 0 0.01 0.05 0.1 0.5
kDa
HA
PEDV-N
GAPDH
-55
-55
-35
E
HA-Casp-1 + + + +
PEDV - + + + MOI=0.1
TIME 12 18 24 hr
kDa
HA-infected
PEDV-N
GAPDH-infected
HA-mock infected
GAPDH-mock infected
-55
-55
-35
-55
-35
F
FLAG-GSDMD-FL + + + +
HA-Casp-1 + + + +
PEDV MOI 0 0.01 0.05 0.1
kDa
FLAG
HA
PEDV-N
GAPDH
-55
-35
-55
-55
-35
G
FLAG-GSDMD-FL + + + + + +
HA-Casp-1 + + + + + +
PEDV - + - + - + MOI=0.05
TIME 12 24 36 hr
kDa
FLAG
HA
PEDV-N
GAPDH
-55
-35
-55
-55
-35
H
Cell death %LDH release
30
20
10
0
**
**
FLAG-GSDMD-FL + + + + +
HA-Casp-1 - + + + +
PEDV MOI 0 0 0.01 0.05 1
I
Cell death %LDH release
30
20
10
0
ns
**
*
FLAG-GSDMD-FL + + + + + +
HA-Casp-1 + + + + + +
PEDV - + - + - + MOI=0.05
TIME 12 24 36 hr

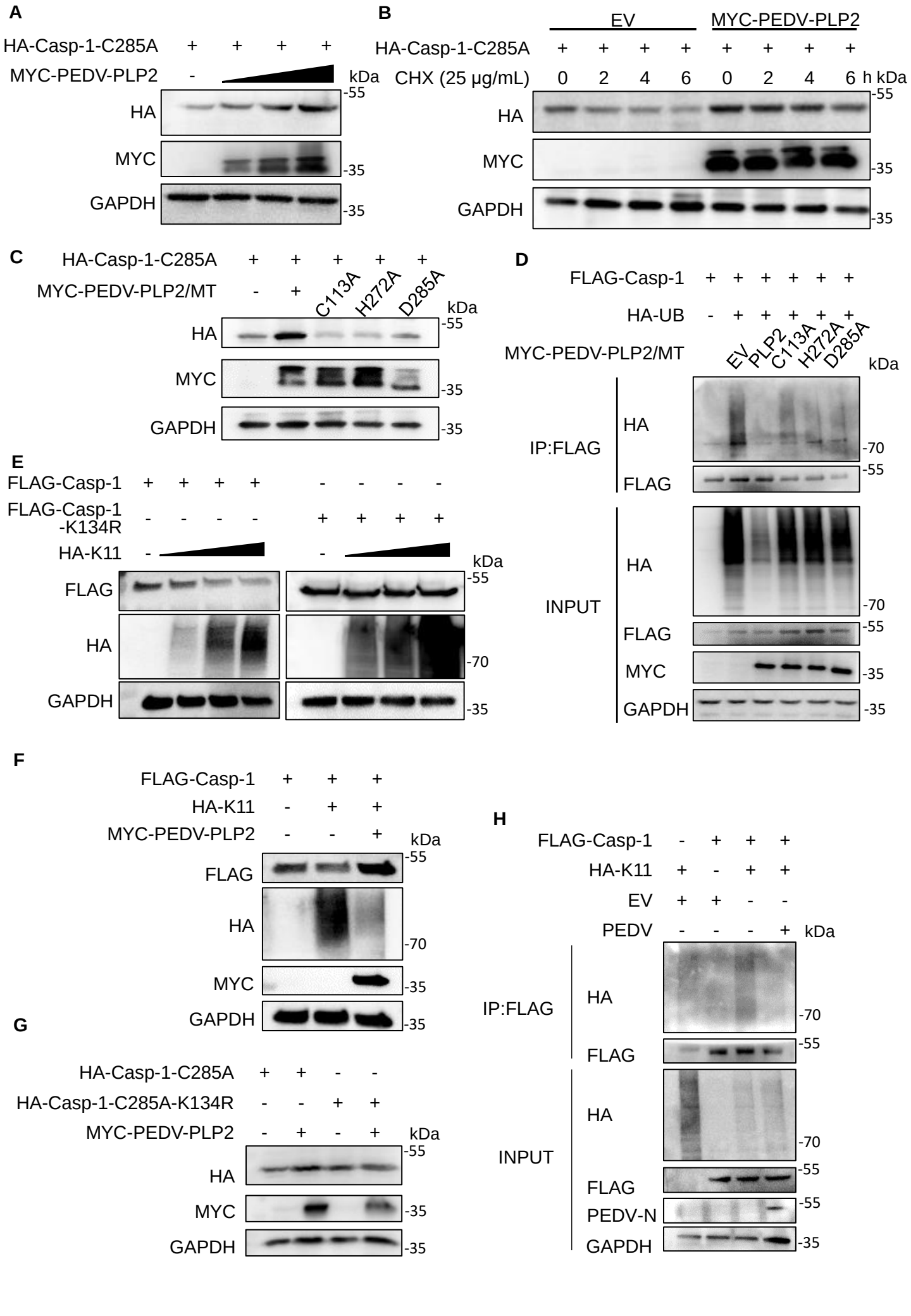
A
HA-Casp-1-C285A + + + +
MYC-PEDV-PLP2 -
kDa
HA
MYC
GAPDH
-55
-35
-35
B
EV
MYC-PEDV-PLP2
HA-Casp-1-C285A + + + + + + + +
CHX (25 μg/mL) 0 2 4 6 0 2 4 6 h
kDa
HA
MYC
GAPDH
-55
-35
-35
C
HA-Casp-1-C285A + + + + +
MYC-PEDV-PLP2/MT - + C113A H272A D285A
kDa
HA
MYC
GAPDH
-55
-35
-35
D
FLAG-Casp-1 + + + + + +
HA-UB - + + + + +
MYC-PEDV-PLP2/MT EV PLP2 C113A H272A D285A
kDa
IP:FLAG
HA
FLAG
INPUT
HA
FLAG
MYC
GAPDH
-70
-55
-70
-55
-35
-35
E
FLAG-Casp-1 + + + + - - - -
FLAG-Casp-1 -K134R - - - - + + + +
HA-K11 - -
kDa
FLAG
HA
GAPDH
-55
-70
-35
F
FLAG-Casp-1 + + +
HA-K11 - + +
MYC-PEDV-PLP2 - - +
kDa
FLAG
HA
MYC
GAPDH
-55
-70
-35
-35
G
HA-Casp-1-C285A + + - -
HA-Casp-1-C285A-K134R - - + +
MYC-PEDV-PLP2 - + - +
kDa
HA
MYC
GAPDH
-55
-35
-35
H
FLAG-Casp-1 - + + +
HA-K11 + - + +
EV + + - -
PEDV - - - +
kDa
IP:FLAG
HA
FLAG
INPUT
HA
FLAG
PEDV-N
GAPDH
-70
-55
-70
-55
-55
-35

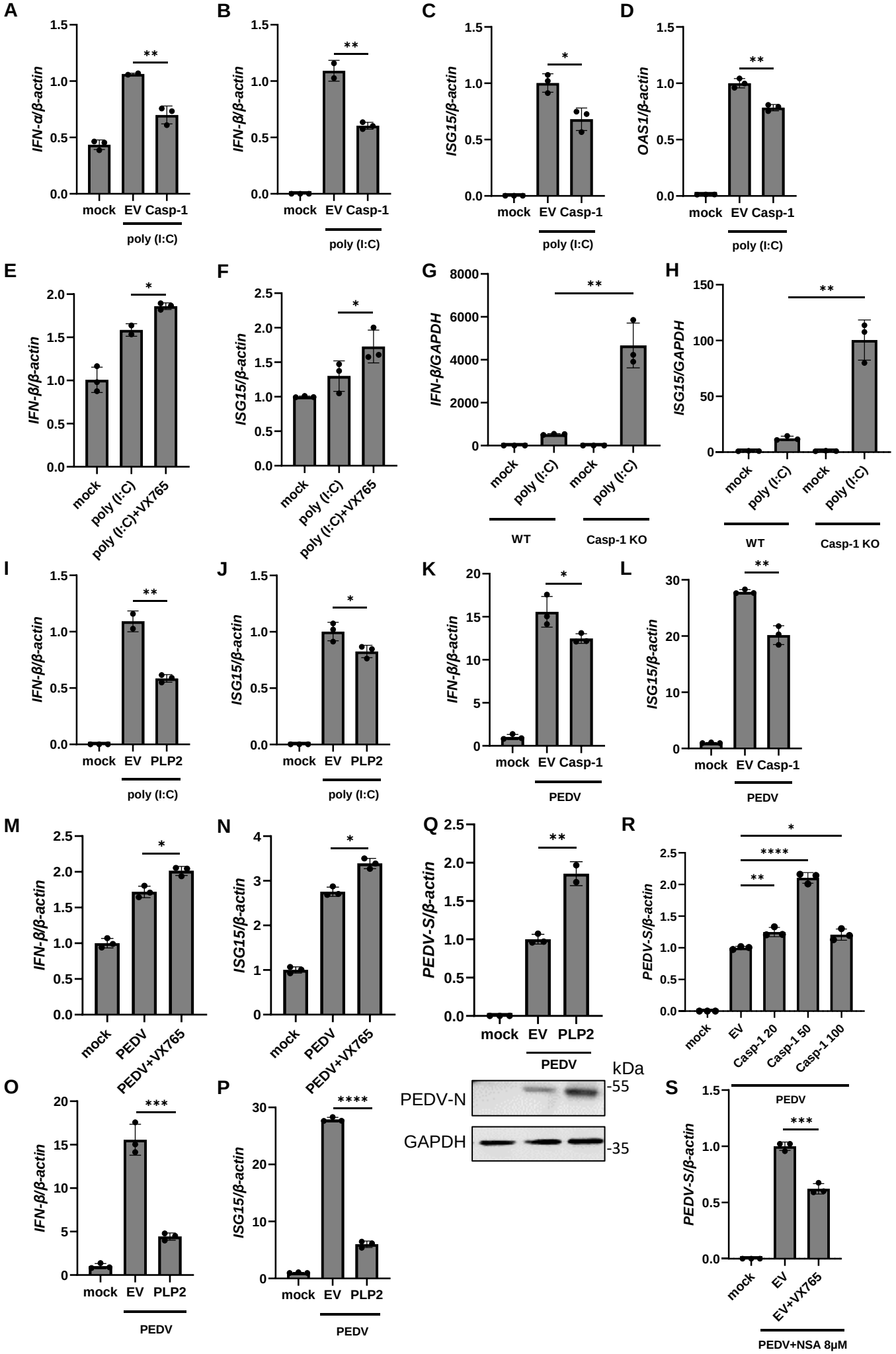
A
IFN-α/β-actin
mock
EV
Casp-1
poly (I:C)
B
IFN-β/β-actin
C
ISG15/β-actin
D
OAS1/β-actin
E
IFN-β/β-actin
poly (I:C)+VX765
F
ISG15/β-actin
G
IFN-β/GAPDH
WT
Casp-1 KO
H
ISG15/GAPDH
I
IFN-β/β-actin
PLP2
J
ISG15/β-actin
K
IFN-β/β-actin
PEDV
L
ISG15/β-actin
M
IFN-β/β-actin
PEDV
PEDV+VX765
N
ISG15/β-actin
Q
PEDV-S/β-actin
R
PEDV-S/β-actin
Casp-1 20
Casp-1 50
Casp-1 100
kDa
PEDV-N
-55
GAPDH
-35
O
IFN-β/β-actin
P
ISG15/β-actin
S
PEDV-S/β-actin
EV+VX765
PEDV+NSA 8μM

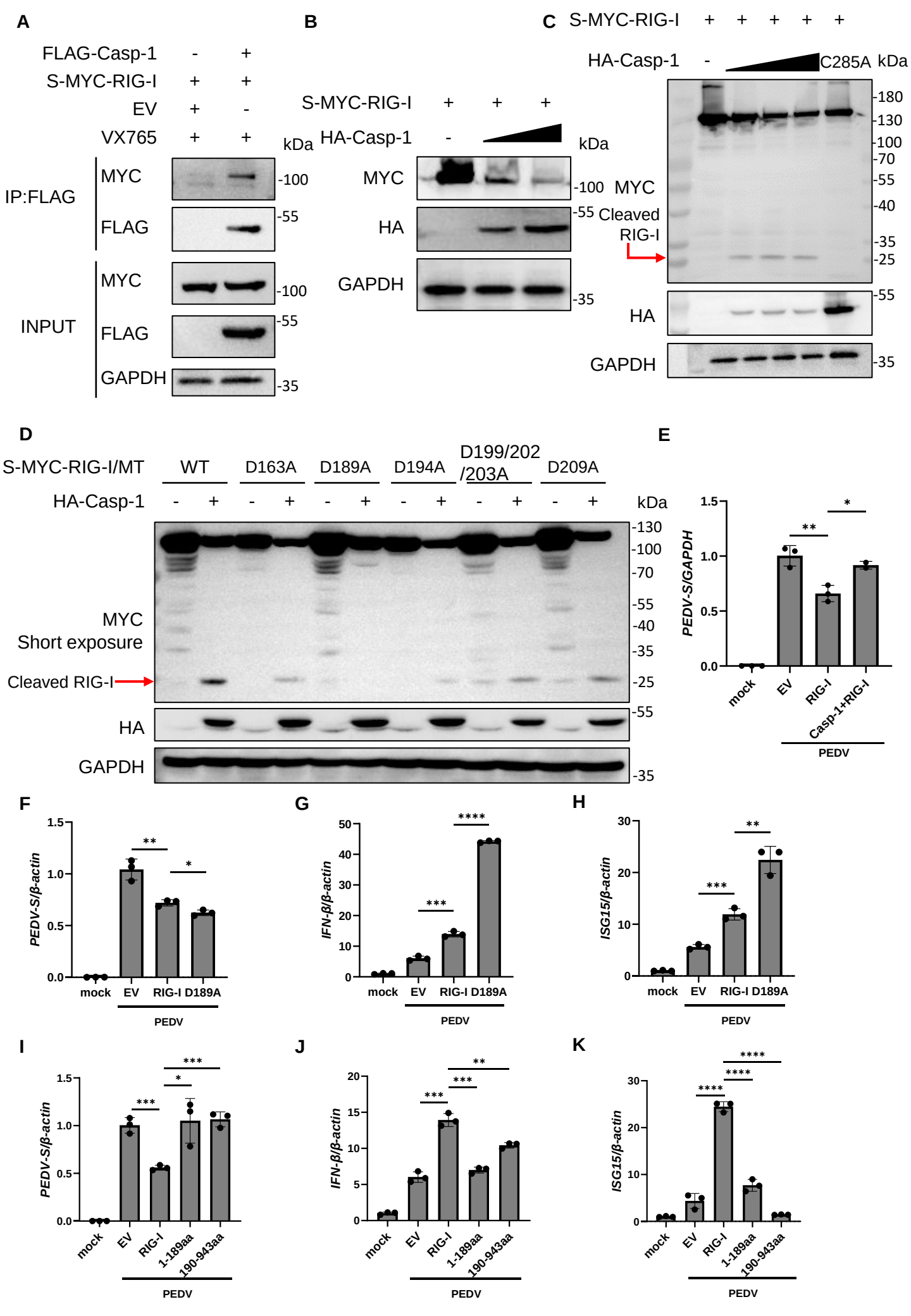
A
FLAG-Casp-1 - +
S-MYC-RIG-I + +
EV + -
VX765 + +
kDa
IP:FLAG
MYC
FLAG
INPUT
MYC
FLAG
GAPDH
-100
-55
-100
-55
-35
B
S-MYC-RIG-I + + +
HA-Casp-1 -
kDa
MYC
HA
GAPDH
-100
-55
-35
C
S-MYC-RIG-I + + + + +
HA-Casp-1 - C285A kDa
MYC
Cleaved RIG-I
HA
GAPDH
180
130
100
70
55
40
35
25
55
35
D
S-MYC-RIG-I/MT WT D163A D189A D194A D199/202/203A D209A
HA-Casp-1 - + - + - + - + - + - + kDa
MYC Short exposure
Cleaved RIG-I
HA
GAPDH
130
100
70
55
40
35
25
55
35
E
PEDV-S/GAPDH
mock EV RIG-I Casp-1+RIG-I
PEDV
F
PEDV-S/β-actin
mock EV RIG-I D189A
PEDV
G
IFN-β/β-actin
mock EV RIG-I D189A
PEDV
H
ISG15/β-actin
mock EV RIG-I D189A
PEDV
I
PEDV-S/β-actin
mock EV RIG-I 1-189aa 190-943aa
PEDV
J
IFN-β/β-actin
mock EV RIG-I 1-189aa 190-943aa
PEDV
K
ISG15/β-actin
mock EV RIG-I 1-189aa 190-943aa
PEDV

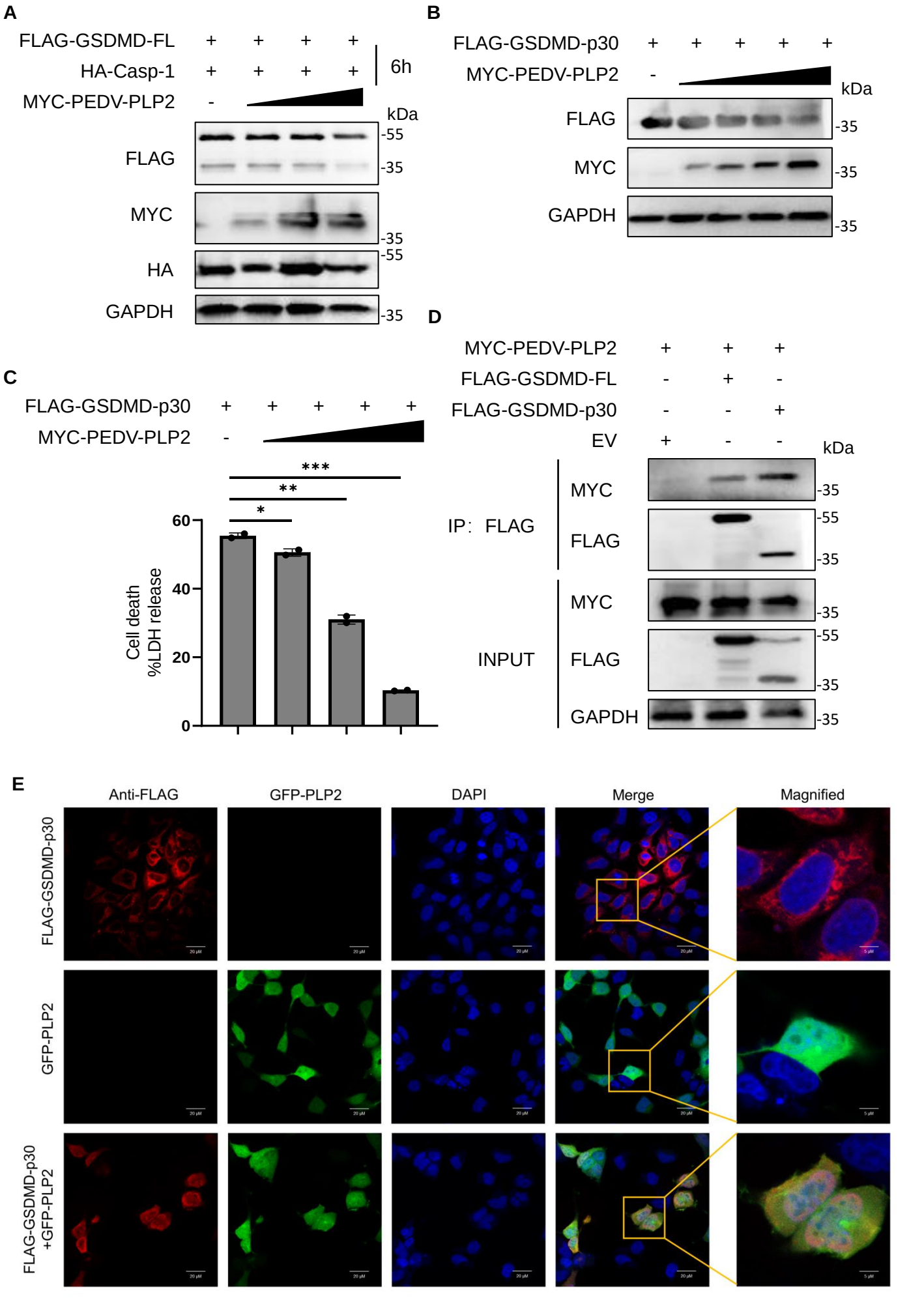
A
FLAG-GSDMD-FL + + + +
HA-Casp-1 + + + +
6h
MYC-PEDV-PLP2 -
kDa
FLAG
-55
-35
MYC
-35
HA
-55
GAPDH
-35
B
FLAG-GSDMD-p30 + + + + +
MYC-PEDV-PLP2 -
kDa
FLAG
-35
MYC
-35
GAPDH
-35
C
FLAG-GSDMD-p30 + + + + +
MYC-PEDV-PLP2 -
***
**
*
Cell death
%LDH release
60
40
20
0
D
MYC-PEDV-PLP2 + + +
FLAG-GSDMD-FL - + -
FLAG-GSDMD-p30 - - +
EV + - -
kDa
IP: FLAG
MYC
-35
FLAG
-55
-35
INPUT
MYC
-35
FLAG
-55
-35
GAPDH
-35
E
Anti-FLAG
GFP-PLP2
DAPI
Merge
Magnified
FLAG-GSDMD-p30
GFP-PLP2
FLAG-GSDMD-p30
+GFP-PLP2

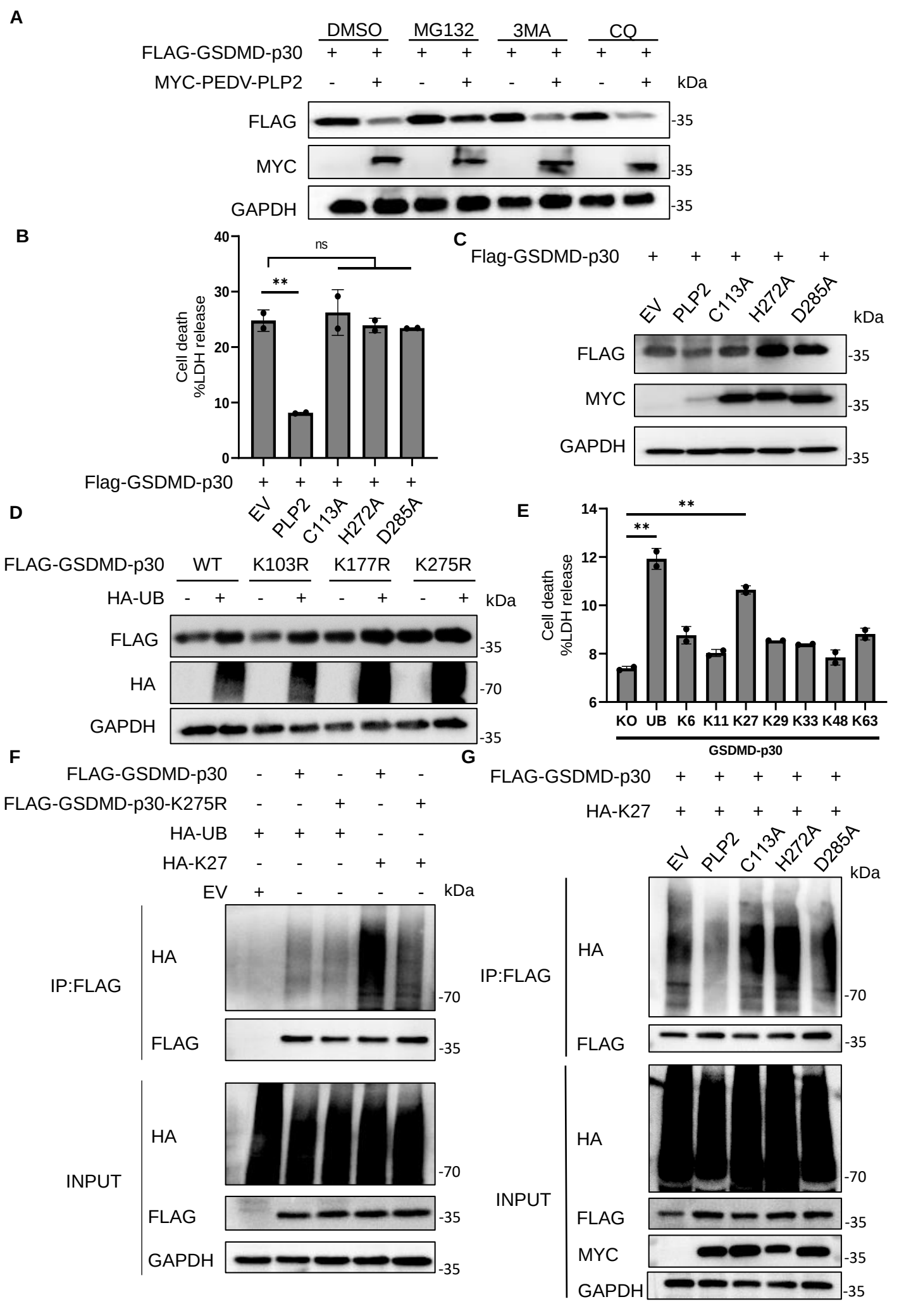
A
DMSO
MG132
3MA
CQ
FLAG-GSDMD-p30
MYC-PEDV-PLP2
kDa
FLAG
MYC
GAPDH
-35
B
Cell death
%LDH release
ns
**
Flag-GSDMD-p30
EV
PLP2
C113A
H272A
D285A
C
Flag-GSDMD-p30
EV
PLP2
C113A
H272A
D285A
kDa
FLAG
MYC
GAPDH
-35
D
FLAG-GSDMD-p30
WT
K103R
K177R
K275R
HA-UB
kDa
FLAG
HA
GAPDH
-35
-70
E
Cell death
%LDH release
**
**
KO
UB
K6
K11
K27
K29
K33
K48
K63
GSDMD-p30
F
FLAG-GSDMD-p30
FLAG-GSDMD-p30-K275R
HA-UB
HA-K27
EV
kDa
IP:FLAG
HA
FLAG
INPUT
HA
FLAG
GAPDH
-70
-35
G
FLAG-GSDMD-p30
HA-K27
EV
PLP2
C113A
H272A
D285A
kDa
IP:FLAG
HA
FLAG
INPUT
HA
FLAG
MYC
GAPDH
-70
-35

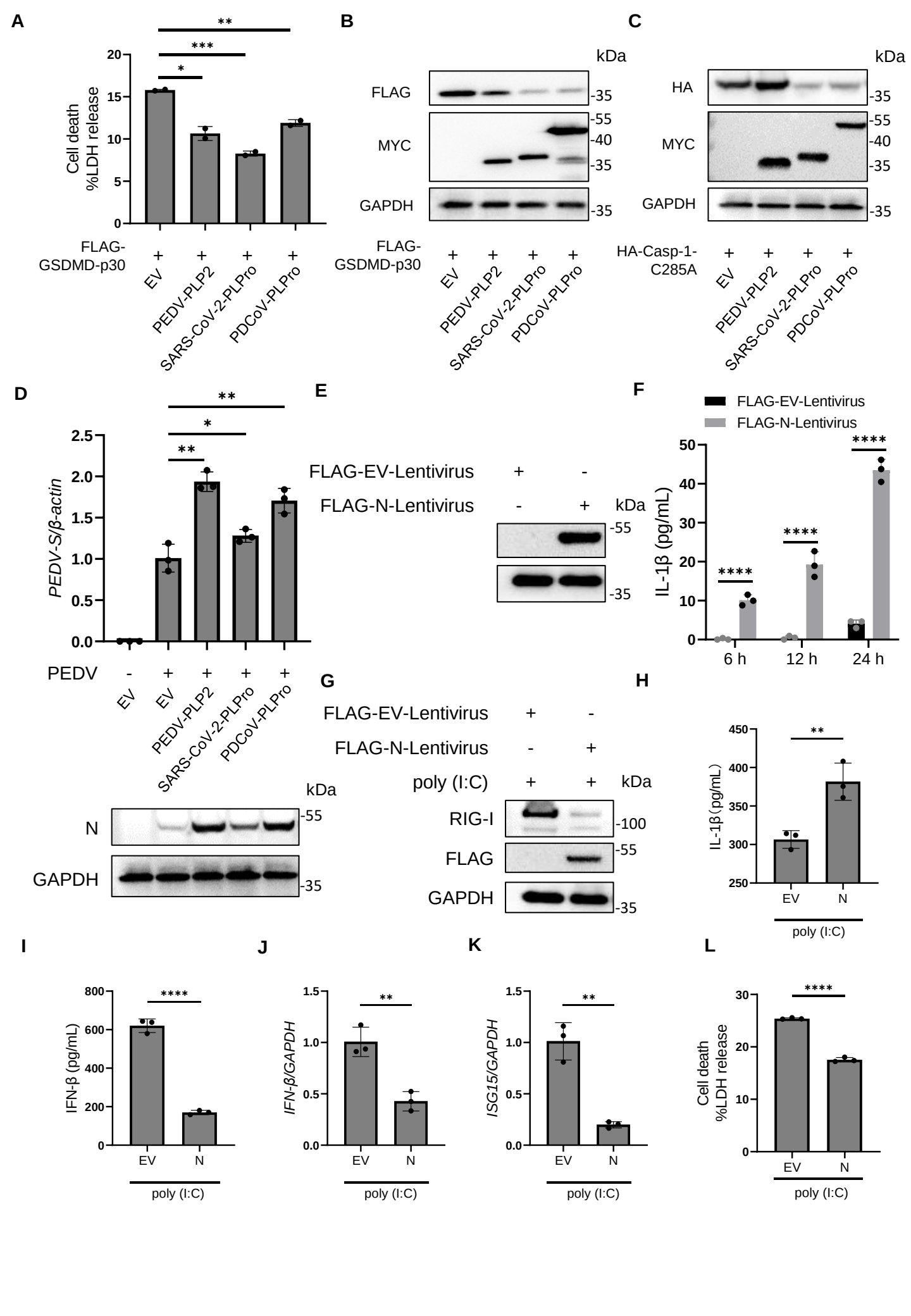
A
B
C
D
E
F
G
H
I
J
K
L
Cell death %LDH release
FLAG-GSDMD-p30
EV
PEDV-PLP2
SARS-CoV-2-PLPro
PDCoV-PLPro
kDa
FLAG
MYC
GAPDH
HA
HA-Casp-1-C285A
PEDV-S/β-actin
PEDV
FLAG-EV-Lentivirus
FLAG-N-Lentivirus
IL-1β (pg/mL)
6 h
12 h
24 h
N
poly (I:C)
RIG-I
IFN-β (pg/mL)
IL-1β(pg/mL)
IFN-β/GAPDH
ISG15/GAPDH

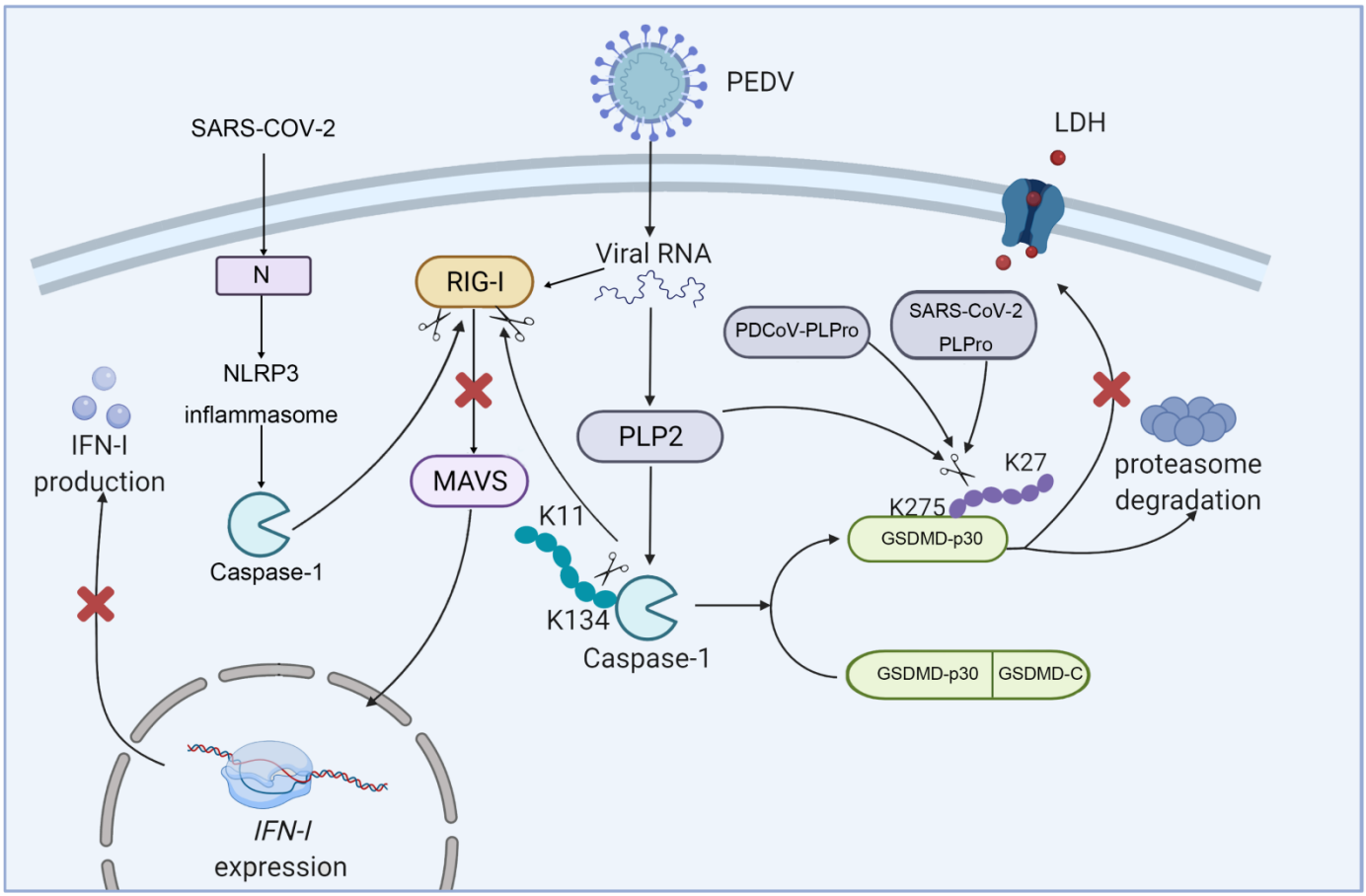
PEDV
SARS-COV-2
LDH
N
RIG-I
Viral RNA
PDCoV-PLPro
SARS-CoV-2
PLPro
NLRP3
inflammasome
IFN-I
production
PLP2
MAVS
K27
K275
proteasome
degradation
K11
GSDMD-p30
K134
Caspase-1
Caspase-1
GSDMD-p30
GSDMD-C
IFN-I
expression